M-AM-Sym-1 The Nature of the Primary Photochemical Events in Rhodopsin and Bacteriorhodopsin

R. R. Birge, T. M. Cooper, C. M. Einterz, L. A. Findsen, M. B. Masthay, L. P. Murray, G. A. Schick, and C. F. Zhang. Department of Chemistry, Carnegie Mellon University, Pittsburgh, PA 15213

Recent experimental and theoretical studies of the binding site geometries and the primary photochemical events in rhodopsin and bacteriorhodopsin will be presented. Our experimental studies included two-photon spectroscopy, pulsed laser photocalorimetry and quantum yield measurements. Our theoretical studies included semiempirical molecular orbital theory and molecular dynamics calculations. Spectroscopic studies indicate that the counterion in rhodopsin is not intimately associated with the imine proton in rhodopsin, but lies underneath the plane of the chromophore. Energy storage associated with the rhodopsin → bathorhodopsin phototransformation is measured to be ~32 kcal mol^{-1} and is partitioned theoretically to involve ~60% conformational distortion and ~40% charge separation. Energy storage associated with the isorhodopsin → bathorhodopsin phototransformation is measured to be ~27 kcal mol^{-1}. Absolute quantum yield measurements of the isorhodopsin to bathorhodopsin phototransformation at 77K indicate a wavelength dependence that ranges from 0.089±0.021 at 565nm to 0.168±0.012 at 440nm. We attribute this result to the presence of a small activation barrier (~0.2 kcal mol^{-1}) in the 9-cis → 9-trans excited state surface. The absence of a wavelength dependence in the rhodopsin → bathorhodopsin photoreaction indicates a barrier-less photoprocess. Two-photon studies indicate that the binding site of bacteriorhodopsin is more "ionic" than that of rhodopsin. Theoretical calculations suggest the possibility that the J intermediate may be an excited state species, which is generated due to the trapping of photoactivated molecules in a 13-transoid minimum in the excited state surface. Photocalorimetry and photostationary state investigations of light adapted bacteriorhodopsin at 77K indicate that the ratio of the forward (Φ_1) to reverse (Φ_2) quantum yields is $\Phi_1/\Phi_2 = 0.445 \pm 0.031$. We conclude that the forward quantum yield must be less than 0.5.

M-AM-Sym-2 STRUCTURE AND FUNCTION OF THE RETINAL CHROMOPHORE IN RHODOPSINS.

R. A. Mathies, Chem. Dept., Univ. of Calif., Berkeley, CA; R. G. Griffin, Francis Bitter National Magnet Lab, MIT, Cambridge, MA; C. V. Shank, AT & T Bell Labs, Holmdel, NJ; J. Hertzfeld, Chem. Dept., Brandeis Univ., Waltham, MA; and J. Lugtenburg, Chemistry Department, Leiden University, 2300 RA Leiden, The Netherlands.

The retinal prosthetic group plays a central role in information transduction by the visual pigment rhodopsin, and in energy transduction by bacteriorhodopsin. Resonance Raman, solid-state ^{13}C-NMR, femtosecond (10^{-15} s) transient absorption and retinal analogue studies have provided a great deal of information about the structure and photochemical dynamics of the retinal chromophore in these pigments. The red shift of the chromophore absorption spectrum maximum upon protein binding is called the opsin shift. Retinal analogue and solid-state NMR studies on rhodopsin and bacteriorhodopsin reveal the relative roles of conformational alteration, hydrogen-bonding changes, and point-charge perturbations in generating the opsin shift. The photochemical dynamics of bacteriorhodopsin have been examined with femtosecond spectroscopy. Excited-state absorption transients are observed which appear to directly monitor the ~200 fs excited state isomerization process. The absorption and stimulated emission signals are consistent with the ~450 fs formation time of the primary ground state product, J. Finally, the structures of the primary photoproducts in rhodopsin and bacteriorhodopsin have been studied with resonance Raman spectroscopy. The mechanism of the 30 kcal/mole energy storage in the primary photoproduct of rhodopsin will be examined. Also, a detailed study of chromophore structure in the photointermediates of bacteriorhodopsin indicates that the proton-pumping mechanism involves C_{13}=C_{14} *cis*, C_{14}-C_{15} s-*trans* chromophore structures.

M-AM-Sym-3 REGULATION OF THE SPECTROSCOPIC AND PHOTOCHEMICAL PROPERTIES OF RETINAL PROTEINS

Thomas G. Ebrey, Dept. of Physiology and Biophysics, University of Illinois, Urbana, Il 61801

Many biophysical techniques have been used to investigate how the apoprotein modulates the spectroscopic, photochemical, and physiological properties of retinal binding proteins. Three pigments, bovine rhodopsin, octopus rhodopsin, and bacteriorhodopsin, will be discussed in detail along with more limited data on cone pigments. The binding sites of these pigments have been studied with stericially-modified retinals, with retinals containing spectroscopic reporter groups, and with vibrational spectroscopy as well as with chemically modified apoproteins. These studies give specific models of the chromophore's binding site and how its absorption spectrum is modulated by surrounding charged groups of the apoprotein. The primary photochemical transformation in all the retinal pigments seems to be cis/trans isomerization. The apoprotein controls the quantum efficiency of the photochemical transformation and the composition of the final products, as well as the ability of the retinal protein to store part of the photon's energy in its primary photoproduct. Many of the retinal proteins go through an intermediated step in their photochemical transformation in which the Schiff base chromophore linkage is deprotonated. This step seems to be required for these pigments to yield their stored energy in a useful way. At the level of physiological action, the retinal pigments start to diverge. There is good evidence that vertebrate rhodopsin can activate a GTP binding protein which then goes on to release an inhibitory constraint from a phosphodiesterase, leading to control of cGMP concentration. Much less is known about invertebrate rhodopsin action, except that a GTP binding protein can be activated by light. In bacteriorhodopsin light is used to move protons across the cell membrane. The requirements on the chromophore to allow for proton movement are stricter than for just binding or even photochemical activity.

M-AM-Sym-4 **AN EVOLUTIONARY COMPARISON OF VISUAL PIGMENTS.** M.L. Applebury, Depts. Ophthalmology and Visual Science and Pharmacological and Physiological Sciences, University of Chicago, Chicago, IL 60637.

The characterization of genes and cDNAs encoding visual pigments have shown that there are striking similarities among all eucaryotic photoreceptors. Relationships are seen in gene structures, general protein domains, and specific segments of amino acid sequences. Inspection of the homologies suggests potential domains that may be important in general receptor folding, an extracellular domain of unknown function, and cytoplasmic domains that may specify the interactions with GTP-binding proteins. Moreover, the opsins are a subfamily of the signal receptors. The latter superfamily is composed of the ligand-mediated receptors which catalyze the activation of GTP-binding proteins. These receptors include the opsins, the β-adrenergic, the muscarinic, serotonin, and Hmas receptors. The relationships observed in some aspects of structure and specific amino acid segments suggest signal receptors may share a general mechanism for ligand-triggered transmembrane signaling.

M-AM-MinI-1 QUANTITATIVE FOOTPRINTING ANALYSIS OF DRUG-DNA INTERACTIONS by Ward, B., Rehfuss, R., Kissinger, K., Goodisman, J. and Dabrowiak, J.C., Department of Chemistry, Syracuse University, Syracuse, New York 13244-1200.

A method for obtaining drug binding constants as a function of sequence from footprinting data using the minor groove binding antiviral agent netropsin, a 139 base pair segment of pBR 322 DNA and two cleaving agents, DNase I and a cationic manganese porphyrin complex will be illustrated. The analysis requires the reduction of autoradiographic data to a series of "footprinting plots" showing the apparent probe cleavage rate as a function of drug concentration and sequence. After accounting for probe redistribution effects as binding sites accept drug (enhancements) and addressing exclusions due to overlapping drug binding sites on DNA, the footprinting plots and the total drug concentration are used in a minimization approach to calculate drug binding constants. The analysis revealed that the high affinity netropsin sites, all of type $(A \cdot T)_4$, have binding constants in the range 10^6-10^8 M^{-1}. Tetranucleotide sites possessing the lowest affinities contained the dinucleotide 5'-TA-3', suggesting that an adenine-adenine clash associated with this sequence may discourage netropsin binding to DNA.

M-AM-MinI-2 RNA STRUCTURES FORMING HIGH AFFINITY INTERCALATION SITES. David E. Draper and Susan A. White, Department of Chemistry, Johns Hopkins University, Baltimore, MD 21218.

Using the intercalating cleavage reagent methidiumpropyl EDTA-Fe (MPE-Fe), we detected the presence of two sites with unusually high affinity for intercalators in a fragment of ribosomal RNA (Biochemistry 24, 5062 (1985)). One site is located in a large bulge loop and is probably formed by RNA tertiary structure. We have prepared RNA fragments with altered sequences in this region but do not yet know the precise structure of the intercalation site. The second site is located at a CpG sequence in a double helix; to one side is a bulged A and to the other side G-A base pairs. Deletion of the bulged base weakens MPE-Fe binding by a factor of about four.

To further explore the effects of a single base bulge on ethidium intercalation into helices, we have prepared a series of hairpin helices containing seven or nine base pairs and single base bulges at various positions. Bulges enhance ethidium binding to these hairpins by as much as an order of magnitude. Our results so far support three generalizations: i) CpG is a preferred sequence for ethidium binding in a regular helix; ii) enhancement of intercalation by a single base bulge is independent of the chemical identity of the bulged base; iii) the bulge can be located at several positions relative to the intercalation site and still affect intercalation. We suggest that when CpG adopts an optimum conformation for ethidium intercalation, stacking interactions between neighboring bases are perturbed. The presence of an extra sugar-phosphate unit associated with a bulge may then allow the helix greater flexibility in adopting a conformation maximizing base stacking interactions. In support of this, we find that ethidium induces dramatic changes in helix conformation several bases distant from the intercalation site in helices containing a bulge.

M-AM-MinI-3 QUANTITATIVE DNase I FOOTPRINTING STUDIES OF THE DAUNOMYCIN-DNA INTERACTION. J. B. Chaires, J. E. Herrera and M. J. Waring*, Department of Biochemistry, The University of Mississippi Medical Center, Jackson, MS 39216-4505 and *Department of Pharmacology, Cambridge University, Cambridge CB2 2QH, England.

Daunomycin is an anthracycline antibiotic of clinical importance in cancer chemotherapy. Daunomycin binds to DNA by intercalation, an interaction that is thought to be a crucial step in the mechanism by which it inhibits transcription and DNA replication in the cell. We have established, through equilibrium binding and DNase I footprinting studies, that daunomycin binds to preferred sites along the DNA lattice (Chaires et al. (1987) BIOCHEMISTRY, in press). The preferred sites appear to be triplet sequences, comprised of adjacent GC base pairs flanked by an AT base pair. We report here more refined DNase I footprinting experiments aimed at defining the preferred daunomycin binding site in more detail. We have obtained DNase I footprinting patterns for binding sites on the 160 bp tyr t DNA fragment over a wide range of total daunomycin concentrations. Microdensitometry provides quantitative estimates of individual band areas as a function of daunomycin concentration from experimental autoradiograms. Individual band intensities are found to vary with daunomycin concentration in unique ways. Our methods for the quantitative analysis of this primary data will be presented, and our progress toward ranking the relative affinity of the multiple daunomycin binding sites within the tyr t DNA fragment will be discussed.
Supported by National Cancer Institute Grant CA35635 and NSF Grant INT-8521004.

M-AM-MinI-4 CORRELATIONS BETWEEN LIGAND STRUCTURE AND DNA BINDING THERMODYNAMICS: THE COMPLEXATION OF NETROPSIN ANALOGUES WITH THE POLY dAT•POLY dAT DUPLEX. Gorazd Vesnaver, J. William Lown,[†] and Kenneth J. Breslauer. Department of Chemistry, Rutgers University, New Brunswick, NJ 08903, [†]Department of Chemistry, University of Alberta, Edmonton, Alberta, Canada T6G 2G2.

We are interested in developing an understanding of the molecular recognition patterns that dictate and control the binding affinities and sequence specificities of DNA binding ligands. Our approach consists of determining thermodynamic binding profiles and interpreting these macroscopic data in terms of specific ligand-DNA molecular interactions. We have employed a combination of spectroscopic and calorimetric techniques to characterize thermodynamically the binding to poly dAT•poly dAT of a series of netropsin analogues in which the structures have been systematically altered. This approach enables us to evaluate how the type and the location of structural features within the ligand influence its DNA binding affinity and specificity. The netropsin analogues investigated in this work have allowed us to assess the thermodynamic consequences of changing the following ligand properties; (1) reducing the charge from +2 to +1; (2) replacing one or both pyrrole rings by imidazole rings; (3) repositioning the pyrrole and the imidazole rings relative to the charged amidinium terminal group; (4) reducing the number of methylene groups linking the charged amidinium group to the adjacent pyrrole ring. The thermodynamic data obtained form these studies will be presented. When possible, these DNA binding profiles will be compared with expectations based on the current structural model of netropsin-DNA interactions. This work was supported by NIH GM34469 (KJB).

M-AM-MinI-5 NMR ANALYSIS OF THE INTERACTION OF ACTINOMYCIN D WITH OLIGODEOXYRIBONUCLEOTIDES CONTAINING MULTIPLE GC BINDING SITES. W. David Wilson and Robert L. Jones, Department of Chemistry, Georgia State University; Gerald Zon, Applied Biosystems; Elwood V. Scott and Luigi G. Marzilli, Department of Chemistry, Emory University.

The interactions of actinomycin D (ActD) with oligodeoxyribonucleotides containing multiple GC and CG sites and flanking AT regions have been investigated by ^{1}H and ^{31}P NMR spectroscopy. With oligomers of the type d(TA)nCGCG(TA)n or d(TA)nTGCA(TA)n, ActD binds at the central GC site. Long range effects of binding are observed in the flanking AT sequences and these effects are not the same in the two oligomers. With the oligomer dATGCATGCAT multiple 1:1 and 2:1 (ActD:oligomer) complexes are seen due to the different binding modes of the asymmetric phenoxazone ring of ActD. With oligomers containing two adjacent GC sites, such as dATGCGCAT, two 1:1 and a unique 2:1 complex are obtained on addition of ActD. In the favored 1:1 and the 2:1 complex the orientation of the phenoxazone ring places the benzenoid side of the ring over the G base in the central base pair of the oligomer. 2D NMR experiments indicate that the two cyclic peptides on an ActD molecule are not in the same conformation in the 2:1 complex. There is considerable anticooperativity in binding of the second ActD in the 2:1 complex. Anticooperativity is also seen in ActD binding to oligomers containing three and four adjacent GC sites. Only two ActD can bind in any consecutive sequence of three GC sites in these oligomers. The complexity of ActD binding modes to natural DNA can be appreciated from these results with oligomers of simpler sequence.

M-AM-MinI-6 Specificity in the Interaction of Drugs and Carcinogens in Binding to DNA. Thomas R. Krugh Department of Chemistry University of Rochester, Rochester, N.Y.

The adducts formed between drugs(such as anthramycin), carcinogens (BPDE and AAAF) with DNA is exhibited in the interaction of these ligands with oligodeoxynucleotides. This provides the opportunity to determine the conformation of the adduct and the DNA at the site of adduct formation. A summary of the results to date will be presented.

M-AM-MinII-1 STRUCTURAL, FUNCTIONAL AND GENETIC STUDIES OF INVERTEBRATE HEMOGLOBINS.
Austen F. Riggs, Kenzo Fushitani and Sissy M. Jhiang. Department of Zoology, University of Texas, Austin, Texas 78712

Hemoglobins are widely but sporadically distributed in most invertebrate phyla. Most of these have hemoglobins of 15-17 kd and are either intracellular (molecules $\leq$ 65 kd) or extracellular with molecular weights to several million. Some hemoglobins of molluscs and arthropods have 2-20 myoglobin-like units joined by peptide bonds. Many hemoglobins exhibit highly cooperative O_2 binding and are strongly affected by pH. Others are non-cooperative and independent of pH. This extraordinary diversity of both form and function provides an attractive system in which to investigate gene structure and evolution and the molecular basis of function. The hemoglobin of the oligochaete earthworm, Lumbricus terrestris, with $\sim$200 subunits has received particular scrutiny. The amino acid sequences of the 4 major chains, a, b, c, and d together with the arrangement of the disulfide bonds indicates that chains a, b and c form a disulfide linked trimer; chain d has only a single intra-chain disulfide. Comparison with the structure of the hemoglobin of the polychaete, Tylorrhynchus heterochaetus, shows that the number and positions of all cysteinyl residues have been conserved since the divergence of oligochaetes and polychaetes. The structure of the gene coding for chain c has been found to have the same intron-exon organization as that found in the genes for vertebrate globins: the splice junctions have been strictly conserved for at least 600 million years. Similar studies are being carried out on the gene structures of two bivalve molluscs that have multiple myoglobin-like domains in single chains.
Supported by NIH Grant GM35848, the Robert A. Welch Foundation Grant F-213 and NSF Grant DMB8502857.

M-AM-MinII-2 QUATERNARY STRUCTURE OF ANNELID EXTRACELLULAR HEMOGLOBINS AND CHLOROCRUORINS.
Serge N. Vinogradov, Mark G. Mainwaring, Daniel A. Walz and Oscar H. Kapp, Biochemistry and Physiology Departments, Wayne State University School of Medicine, Detroit MI 48201 and Enrico Fermi Institute, University of Chicago, Chicago IL 60637.
The hemoglobin of Lumbricus terrestris, M_r = 3.8 x 10^6, consists of four subunits, M (17 kDa, chain I), D1 (31 kDa, chain V), D2 (37 kDa, chain VI) and T (50 kDa, disulfide-bonded trimer of chains II, III and IV). A recently proposed "bracelet" model of the quaternary structure of Lumbricus hemoglobin (Vinogradov et al., PNAS 83, 8034, 1986) was provided with additional support from a study of the chlorocruorin of Eudistylia vancouverii which has approximately the same electron microscopic dimensions and consists of two subunits, D (31 kDa) and T (ca. 65 kDa, disulfide-bonded tetramer of four chains of ca. 16 kDa). The dimer subunit of the chlorocruorin aggregates at neutral pH. The products of this aggregation when examined by STEM are found to be ring structures, uniform in size, ca. 10 nm in diameter. Similar structures have been observed in STEM studies of repeated dissociation of Lumbricus hemoglobin. These results indicate that the D subunits have a capacity for self-association into circular structures. In addition, the subunit stoichiometry in Lumbricus hemoglobin and in Eudistylia chlorocruoroin were determined from quantitative amino acid analyses of the individual subunits of the two molecules separated by SDS PAGE. (Supported by NIH grants DK 38674 and AM 30382 and a grant from the Department of Energy).

M-AM-MinII-3 THE CRYSTAL STRUCTURE OF LUMBRICUS ERYTHROCRUORIN.
William E. Royer, Jr. and Wayne A. Hendrickson, Howard Hughes Medical Institute, Dept. of Biochemistry & Molecular Biophysics Columbia University, NY, NY 10032

Erythrocruorin is a 3.9 x 10^6 dalton respiratory protein found freely dissolved in the blood of various annelids. We are investigating the structure of Lumbricus terrestris erythrocruorin to learn the bases for its self-limited assembly from a few kinds of myoglobin-sized polypeptide chains. We have grown four different crystal forms, one of which (type III) we are using for a structural investigation. In this form, the molecule lies on a crystallographic dyad axis of space group $C222_1$ (a=502.1A, b=297.8A, c=350.1A); thus the asymmetric unit of the crystal comprises a half molecule. We have measured diffraction data out to Bragg spacings of 5.5A using synchrotron radiation from the sources at Stanford and Cornell. Self rotation functions calculated from these data demonstrate that the whole molecule has D_6 symmetry to a resolution of 5.5A. They also show that the molecule lies in the crystal with a molecular two-fold axis coincident with the a axis and the hexagonal face tilted by 15° from the ab plane. With the orientation known, the only unknown would be the position of the molecular center along the a axis. Packing considerations restrict this position to a point near a=¼. With this information and recently obtained EM reconstruction kindly supplied by Drs. Marin van Heel and Egbert Boekema (Fritz-Haber Institute, Berlin) we can begin to phase the innermost reflections (spacings greater than 20A), and then to use 6-fold symmetry averaging to extend to phasing.

M-AM-MinII-4 STRUCTURAL AND FUNCTIONAL STUDIES OF THE HEMOGLOBINS FROM ARCID MOLLUSCS

Emilia Chiancone CNR Center of Molecular Biology, Department of Biochemical Sciences, University 'La Sapienza', 00185 Rome, Italy.

The two hemoglobins contained in the red cells of the Arcid mollusc Scapharca inaequivalvis are intriguing since they provide the first proof that cooperativity in ligand binding may be achieved by means of different modes of assembly of globin chains.

HbI, a homodimer, is unique in that the heme-linked E and F helices are not exposed to solvent as in vertebrate hemoglobins, but face eachother and form the intersubunit contact; in HbII two such dimers constructed from unlike chains form a tetramer. "Sticky patches" for dimer assembly are provided by several hydrophobic residues which are not present in the E and F helices of vertebrate globins. As to the heme site, two histidines provide the proximal and distal heme ligands; in the deoxygenated derivative the proximal His-Fe bond is strained as indicated by a number of spectroscopic features.

The unique assembly of S. inaeqivalvis hemoglobins allows cooperativity to be displayed by the homodimeric HbI, while in vertebrate hemoglobins a prerequisite for cooperative ligand binding is the presence of unlike chains in a tetrameric molecule. However, Arcid hemoglobins are not as sensitive to allosteric effectors as vertebrate hemoglobins and in this respect appear as a simpler molecular machinery.

M-AM-MinII-5 CONFORMATIONAL CHANGES OF TARANTULA HEMOCYANIN STUDIED BY FLUORESCENCE LABELLING.

T. Leidescher, H. Decker & B. Linzen, Dept. of Zoology, Univ. of Munich, D-8000 Munich, 2, F.R.G.

The tarantula (Eurypelma californicum) hemocyanin consists of 24 subunits. It is characterized by high cooperativity (nH>7) and a strong Bohr effect (ϕ>-1.0). The binding behavior can be explained on the basis of a modified MWC model, the Nesting model: Hierarchies in structure can be correlated with hierarchies in allosteric function (Robert et al., PNAS (1987) 84: 1891-1895). The smallest structural repeating unit, the 12-mer is assumed to obey the MWC model. Its isologous dimerisation opens a new level of allosteric binding behavior. Conformational transitions were studied by labelling the hemocyanin with a fluorescence tag, NBD chloride. The λ max of fluorescence emission shifted depending on pH and the degree of oxygenation. The λ max of fully oxygenated Hc was 531.5 nm (pH<7.8) and 530.0 nm (pH>7.8). For deoxygenated Hc the values are 533.5 nm (pH <7.2) and 535.0 nm (pH>7.2). The observation of four different emission maxima supports the hypothesis of four conformational species. The relative abundance of each species at different levels of oxygenation was calculated according to the Nesting model and correlated with the transitions in λ max.

M-AM-A1 MICROWAVES FACILITATE DELIVERY OF CARBOXYFLUOROSCEIN FROM LIPOSOMES TO TARGET CELLS.

Robert P. Liburdy, Donna K. Hendrix, Lawrence Berkeley Laboratory, UC Berkeley, Berkeley, CA, Frank J. Martin, Liposome Technology, Inc. Menlo Park, CA

Delivery of drugs from liposomes to different target cell populations was investigated using a fluorescent dye marker to visualize solute transfer. The dye 6-carboxyfluoroscein (CF) was self-quenched inside liposome vesicles comprised of lecithin and also of phospholipids with 16- and 14-carbon chain lengths. Human erythrocytes and lymphocytes, rodent lymphocytes, rodent tumor cells, as well as rodent macrophages were treated with CF-liposomes to promote cell-surface binding. Washed liposome-cell complexes were subsequently exposed to 2450 MHz microwaves or sham-treated at identical temperatures below the phase transition for the liposome system, and dye transfer was assessed visually by microscopy as well as by spectrofluorometric assay. Microwaves facilitated dye transfer compared to that for thermal controls; the extent of dye transfer varied for the cell type. The kinetics and the dependence on field strength, as well as the temperature dependence of this membrane effect is being investigated.

M-AM-A2 MOVEMENT OF RETINOL BETWEEN RETINOL BINDING PROTEIN (RBP) AND UNILAMELLAR VESICLES.

Noa Noy (Intr. by Maria Tomasz), Div. of Digestive Diseases, Cornell University Medical College, New York, NY 10021

Vitamin A which is poorly soluble in water is transported in blood bound to a soluble protein-RBP. In order to reach target sites, retinol has to dissociate from the protein, associate with cellular plasma membranes and translocate across the membranes into the cells. The mechanism of this process is not known, but it is usually suggested that transfer depends on the presence of protein receptors in the plasma membranes of cells. In the present study, the kinetics of the spontaneous transfer of retinol between RBP and unilamellar vesicles of egg PC (ULV) was investigated. Dissociation of retinol from the protein was followed by fluorescence measurements: Excitation of holo-RBP (at 290 nm) results in an energy transfer to retinol, the fluorescence of bound retinol emission at 480 nm can then be observed. Dissociation of the ligand from the protein upon mixing with ULV's was thus monitored by the decrease in retinol fluorescence. Binding of retinol to the protein also results in decrease in the intrinsic fluorescence of RBP itself (excitation - 290 nm, emission - 340 nm). Dissociation of ligand from RBP onto the vesicles was followed also by monitoring the time dependent increase in protein fluorescence which was observed when holo-RBP was mixed with ULV's. The transfer process was found to be biphasic. The faster phase had an apparent rate constant of 0.35/min. The rate of the second, slower phase depended on the concentration of ULV present in the system so that it was faster at higher lipid concentrations. Possible interpretations for these phenomena will be discussed. This work was supported by the American Cancer Society (grant#BC-551).

M-AM-A3 Inhibition of H^+/OH^- Flux across Phospholipid Bilayers by Cholesterol and Low Concentrations of Detergents. Li, W., Haines, T. H., Katz, A. and Avron, M. Dept. Chem., City College of CUNY, NY; and Dept. Biochem., Weizmann Institute, Rehovoth, Israel.

Measurement of the proton/hydroxyl flux across bilayers of uniform, unilamellar, phospholipid vesicles in sizes ranging from 200 nm to 600 nm have been made. Membrane conductivity of H^+/OH^- was assayed by the concentration of acridine orange into vesicles during the impression of a pH gradient of 2.5 - 3.0 units (neutral range, inside low pH) across the bilayer. Vesicles were made of DOPA, DOPC, DOPG, DOPE, DOPG, Escherichia coli lipids, and mixtures of DOPG with sequentially increasing mole fractions of cholesterol, cholic acid, and octyl glucoside, and with plasma membrane vesicles derived from Dunaliella salina. By and large the proton/hydroxyl permeability was found to be that reported by other investigators. Surprisingly, the permeability was reduced by an order of magnitude by increasing the mole% cholesterol from 20 to 30. Low levels of octyl glucoside lowered permeability whereas cholate had essentially no effect. D. salina vesicles had permeability equivalent to that of 30 mole% cholesterol.

M-AM-A4 **OH^- ENHANCES THE CATION CONDUCTANCE OF THE GRAMICIDIN CHANNEL.** G. Eisenman, E. Neher and J. Sandblom. Physiol. Dept., UCLA Med. School, L.A., CA 90024. MPI-fur Biophys. Chem., Gottingen, GFR. Dept. of Med. Phys., U. of Goteborg, Sweden.

The conductance of the gramicidin channel for alkali cations is quite independent of anions like Cl^- F^- Ac^- NO_3^-. The differences in single channel conductance shown in the figure for OH^- vs. Cl^- are therefore surprising. Single channel gramicidin A conductances at 50 mV (G^{50}) for Li^+ and Cs^+ were measured from single openings or from noise in mono-oleate or Eibl's non-hydrolysable mono-oleyl ether (boxes) bilayers. The latter controlled for absence of alkaline hydrolysis. The data for Cl^-, with their accompanying theoretical curves are our published results. The dashed curves for OH^- are not theoretical. Our findings could be explained if the OH^- anion bound near the channel mouth and modulated the energy profile for cation permeation either directly (electrostatically) or indirectly through surface charge effects increasing local concentration of cations. One mechanism for such binding could be by H-bonding to the end of the chain of channel water molecules. Alternatively, it is conceivable that hydration of the peptide carbonyl backbone leads to gem-diol formation changing >C=O groups to $>C(OH)_2$ groups from which either OH^- or H^+ could dissociate.

Supported by USPHS (GM24749) and NSF (BNS8411033).

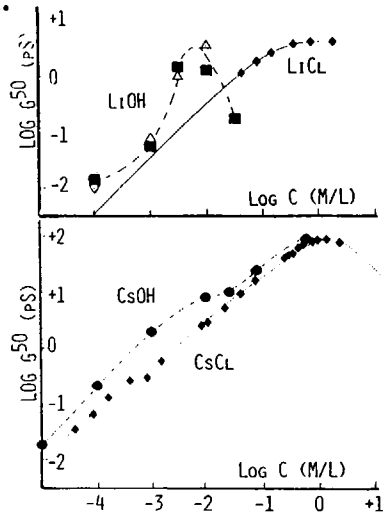

M-AM-A5 CONFORMATION AND ORIENTATION OF GRAMICIDIN A IN ALIGNED PHOSPHOLIPID BILAYERS MEASURED BY SOLID STATE CARBON-13 NMR. B.A. Cornell and F. Separovic, CSIRO P.O. Box 52, North Ryde, N.S.W. 2113, and R. Smith and A.J. Baldassi, University of Queensland, St. Lucia, Queensland 4067. Australia.

A series of analogs of the ionophore gramicidin A has been synthesised with carbon-13 labels at the carbonyl carbons of Leu_{14}, Leu_{12}, Val_7, Ala_3, and Gly_2. These analogs were dispersed at a mole ratio of 1:15 in either ether or ester linked phospholipids and aligned as multilayer stacks on glass cover slips. From the orientation dependence of the solid-state carbon-13 NMR spectrum of the carbonyl groups we have obtained a measure of the reduced chemical shielding anisotropy (CSA) of these nuclei. By comparison with the carbon-13 shielding tensor orientation obtained from model compounds, these CSA's were interpreted in terms of both the order and conformation of the peptide in a number of lipid phases. Axial reorientation of a $\beta^{6.3}$ helix would result in a reduced CSA of approximately -17ppm for the odd numbered residues and -13ppm for the even numbered residues. In the Lα phase of dimyristoyl-phosphatidylcholine the reduced CSA for Ala_3 and Val_7 was 15±1ppm and 16±1ppm respectively. Gly_2, Leu_{12} and Leu_{14} had CSA's of -9±1ppm, -11±1ppm and -13±1ppm. A right-handed helix would result in a reversal of the odd and even numbered assignments for the CSA. Thus a left-handed helix appears the more likely conformation. Other models for the conformation have been unsuccessful. Altering the lipid chainlength from C-10 to C-18 did not produce a significant change in the conformation of the peptide. Cooling the lipid to the Lβ phase caused the peptide to stop rotating on the ms timescale without altering the conformation. Sodium ions perturbed the Leu_{12} and Leu_{14} sited labels. The other sites were unaffected. Gramicidin A appears substantially independent of the state of the surrounding membrane.

M-AM-A6 PEPTIDE BACKBONE DYNAMICS OF GRAMICIDIN A IN LIPID BILAYERS USING SOLID STATE ^{15}N NMR SPECTROSCOPY. L.K.Nicholson, P.V.LoGrasso, C.G. Fields and T.A. Cross. Department of Chemistry and Institute of Molecular Biophysics, Florida State University, Tallahassee, FL 32306-3006

Solid state ^{15}N NMR studies of uniform and specific site ^{15}N labeled gramicidin A in DMPC bilayers have been performed to study the dynamics of the peptide linkages that line the pore of the gramicidin cation channel. Motions of the transmembrane channel have been detected by observing the averaging of the ^{15}N chemical shift anisotrophy (CSA) as a function of temperature in both oriented and unoriented samples.

The temperature dependence of the ^{15}N powder patterns shows that fast overall channel rotation occurs at temperatures in and above the lipid phase transition region, and that below the lipid phase transition region the frequency of this motion is less than the 3kHZ timeframe of the experiment. The coincidence of the resonant frequencies in spectra of oriented samples with the σ_{11} component of the motionally averaged powder patterns shows that the axis of the rotational motion is parallel with the bilayer normal, which is aligned with the magnetic field. The temperature dependence of the ^{15}N spectra of oriented samples shows that local motions exist above the onset of the gel to liquid crystalline phase transition, and that the amplitude of these motions varies from site to site along the peptide backbone. Those experimental results are interpreted as evidence for librational motions that could be responsible for rotating the carbonyl oxygens of the peptide linkages toward the center of the channel pore for solvation of the monovalent cations during cation transport. This work has been supported by NSF (DMB-8451876, DMB-8504250), Procter and Gamble and NIH (AI-23007)

M-AM-A7 **MEASUREMENT OF ALAMETHICIN-MEDIATED ION TRANSLOCATION THROUGH ASYMMETRIC POLYMERIZED LIPID BILAYERS.** **Paul Yager[1] and Keith Seib[2];** [1]Bioengineering, FL-20, University of Washington, Seattle, WA 98195, and [2]Bio/Molecular Engineering Branch, Code 6190, Naval Research Laboratory, Washington DC 20375-5000

We have demonstrated that asymmetric bilayers consisting of one monolayer of polymerized diacetylenic lecithin and the other monolayer consisting of asolectin can support the function of alamethicin, although this function is somewhat modified. In our development of biosensors based on membrane proteins immobilized in polymerized lipid films we have been exploring methods of fabricating polymerized lipid bilayers that avoid irradiation of the protein with ultraviolet light. A monolayer of 1,2-bis-(10,12-tricosadiynoyl)-**sn**-glycero-3-phosphocholine was formed at the air-water interface and polymerized with a low-pressure mercury lamp. Another monolayer was formed from asolectin, and a patch electrode was passed through them using the method of Coronado and Latorre (Biophys. J. 43:231-326 (1983) to form an asymmetric bilayer. Alamethicin presented to the asolectin monolayer formed channels through such bilayers, although the turn-on voltage for the channels was substantially higher and the conductivity lower than for symmetric asolectin bilayers. A model for this behavior will be presented. Membrane stabilization in the form of a substantial increase in the bilayer breakdown voltage was also seen. Some aging of the polymerizable lipid in organic solvent was necessary to allow formation of stable asymmetric bilayers, implying that unknown oxidation products may be necessary contaminants.

M-AM-A8 STRUCTURE-FUNCTION RELATIONSHIPS IN PEPTIDE-INDUCED ION CHANNELS. M.T.Tosteson,L.Capora le* and D.C.Tosteson. Dept.Physiology and Biophysics, Harvard Medical School, Boston MA 02115 and (*) Merck,Sharp & Dohme Research Labs. West Point, PA 19486.

We have used the all L-amino acid peptides melittin and some analogues to test the notion that mono mers of amphipathic peptides aggregate in membranes to form ion-permeable pathways. In the case of melittin, the aggregate is composed of four monomers and the conductance induced in lipid bilayers containing a large number of such aggregates is time- and voltage-dependent. Thus, the conductance of each of the activating regions varies exponentially with voltage, having an apparent gating char ge of 1/4 and 1 per monomer respectively. Replacement of the Lys at position 7 for Asn or blocking of the N-terminus leads to an increased number of monomers in the aggregate (8-9) and to a dramatic change in the time-dependent characteristics, with both the activation and the inactivation being completed in a faster time scale. The apparent gating charge of the 2nd activating region is 1/2-1/3 per monomer for both analogues. These results suggest that the presence of a charge at the N-ter minus or at residue 7 in melittin is not essential for the existance of a time- and voltage-depen-dent conductance. We have also found that the channel conductance of each of these peptides (inclu-ding melittin) is multisized, with differences in the size of the single channel conductance, as well as differences in the kinetic characteristics. These results suggest that amphipathic peptides do aggregate to form ion-permeable pathways, the characteristics of which depend on the primary structure of the peptide in question. The conformation of the monomers and their spatial relations in the aggregate remain a subject of continuing study.

Supported in part by NIH grant GM 25277

M-AM-A9 THE ANTIBIOTIC MAGANIN II FROM THE AFRICAN CLAWED FROG FORMS AN ANION PERMEABLE IONOPHORE IN ARTIFICIAL MEMBRANES. R.A. Cruciani[1], E.F Stanley[2], M. Zasloff[3], D. L. Lewis[1] and J. L. Barker[1], [1]LNP and [2]LB, NINCDS; [3]HG, NICHD, NIH. Bethesda MD. 20892. (Spons. C.A. Colton).

Maganin II (MGII), a 23 amino acid peptide isolated from the skin of African clawed frog *Xenopus Laevis*, exhibits antimicrobial activity against a broad range of microorganisms including gram-positive and gram-negative bacteria, fungi and protozoa (Zasloff, PNAS 84:5449). The mode of action of this antibiotic is not known, although an ionophore structure has been suggested on the basis of computer modeling. We have tested this hypothesis by incorporating MGII into lipid bilayers.

MGII was synthesized from its known amino acid sequence, and was of a high grade of purity. PS:PC:n-decane bilayers were formed on the tips of 3-8 μm glass pipettes and were held under voltage clamp. MGII was incorporated into the bilayer from the internal solution and caused a concentration-dependent increase in the conductivity of the bilayers. The MGII-induced current was voltage dependent, increasing with potential shifts of both polarities, in particular during strong negative potentials. The conductance followed the Cl, and not the K or Na gradient, but appeared to be unselective between Cl and methylsulphonate. Single MGII conductance steps were observed with a wide range in conductance, from 10^{-12} to 10^{-9} S in 100 mM KCl.

These results show that MAG-II forms an anion channel in artificial membranes, presumably by the interaction of a variable number of interacting molecules. This anion ionophore behavior may account for the antibiotic properties of this peptide.

M-AM-A10 INTERACTIONS OF THE CHANNEL FORMING PROTEIN COLICIN B WITH PLANAR LIPID BILAYERS. J.O. Bullock, J.L. Shear, S.K. Armstrong[+], and M.A. McIntosh[+]. Departments of Physiology and Microbiology[+]. University of Missouri. Columbia, MO 65212.

The bactericidal action of one group of colicins, including A, E1, Ia, Ib, and K, results from their ability to form ion channels in the plasma membrane of target cells. Colicin B is a member of this group which has only recently been isolated and purified. In solvent-free planar membranes composed of asolectin, colicin B induces a slow, continuous increase in conductance when trans negative voltages are applied. This conductance is less than ideally selective for Na^+ over Cl^-, the zero current potential having a value of +27.7±1.7 mV for a ten-fold concentration gradient of NaCl at pH 5 and +39.0±0.8 mV at pH 6. The predominant open state observed in single channel records exhibits a conductance of 13.3±1.5 pS at pH 5 in 1M NaCl. In response to trans positive voltages, open channels turn off rapidly at pH 4, but more and more slowly with increasing pH up to pH 7. When negative voltages are restored, the conductance increase exhibits a distinct rapidly activated component in addition to the slow, continuous phase. The number of rapidly activated channels is larger than the number previously turned off by positive voltages. No rapidly activated channels are observed at pH 9. The slow phase of the conductance increase is unaffected by pH in the range from 7 to 5, but it can be markedly slowed or halted by perfusion of the chamber with colicin-free buffer. A mouse antiserum raised against colicin B was found to specifically inactivate the aqueous protein. The antiserum had no effect on open channels or on a population of channels which is membrane associated but unopened. Implications of these findings for the mechanism of channel formation by colicin B will be discussed. (NIH GM 37396 & NSF DBM 8416017).

M-AM-A11 HYPOTHESIS: AN INCREASE IN OSMOLARITY OF SECRETORY VESICLES TRIGGERS EXOCYTOSIS BY REDUCING THE DISTANCE BETWEEN VESICLES AND THE PLASMA MEMBRANE. Gerald Ehrenstein and Elis Stanley, Laboratory of Biophysics, NINCDS, NIH, Bethesda, MD 20892.

Several models attempt to explain the fusion of secretory vesicles with the cell plasma membrane in terms of the establishment of an osmotic gradient across the vesicle membrane. Recent experiments on sea urchin eggs, bovine neurohypophysis, and bovine parathyroid cells are consistent with such an osmotic gradient.

What is the role of the osmotic gradient? In general, previous models have proposed that its role is to cause vesicle swelling, leading to vesicle lysis and subsequent fusion. However, recent experiments on mast cells of beige mice indicate that vesicle swelling occurs after fusion, and, therefore, is not the cause of exocytosis.

We propose another role for the osmotic gradient: to cause water to enter the vesicle from the space between the vesicle membrane and the plasma membrane, thus causing the two membranes to move closer together. We further propose that the probability of fusion of these membranes is a very sensitive function of the distance between them. Thus, a small reduction of this distance caused by the osmotic gradient leads to a large increase in the rate of exocytotic events.

M-AM-A12 FUSION OF SENDAI VIRUS WITH LIPOSOMES AND WITH BIOLOGICAL MEMBRANES: A COMPARISON Debi Prasad Sarkar and Robert Blumenthal, Section on Membrane Structure and Function, LTB, NCI, NIH

We studied fusion between membranes of Sendai virus and liposomes, or human erythrocytes ghosts (HEG) using an assay for lipid mixing based on the relief of self-quenching of octadecylrhodamine (R18) fluorescence. The liposomes were made of phosphatidylcholine (PC), and the effects of including cholesterol (chol), the sialoglycolipid, GD1a, and/or the sialoglycopotein, glycophorin, as receptors were tested. We only considered viral fusion that reflects the biological activity of the viral spike glycoproteins. We used inhibition of Sendai virus-liposome fusion by treatment of the virus with dithiothreitol as a criterion for biological relevance, since such treatment inhibits fusion of Sendai virus with biological membranes. Fusion with HEG occured at a 30-fold faster rate then with PC/chol/Gd1a liposomes; inclusion of glycophorin into the liposomes enhanced the rate 2-fold. We observed no different rates of fusion of Sendai virus between HEG and right side out vesicles derived from HEG, or between liposomes of different sizes ranging from 20 nm to 2000 nm in diameter. Those results indicate that target size did not account for differences in fusion efficiency between biological membranes and lipid model membranes. Prior incubation of Sendai virus with liposomes did not inhibit subsequent fusion with HEG, indicating that the virus-liposome interaction was weak. Fusion of Sendai virus with PC/chol liposomes occured at a 3-fold faster rate than with liposomes composed of PC, PC/GD1a or PC/chol/GD1a. Treatment of HEG with pronase did not affect fusion with Sendai, but treatment with pronase and neuraminidase did inhibit fusion. However, incorporation of GD1a into asialo-HEG restored fusion to the same rate as untreated HEG. Why the biological membranes are much better targets for viral fusion than the liposomes containing the appropriate receptors still remains to be explored.

M-AM-B1 ASSYMETRICAL ION CHANNEL DISTRIBUTION IN TASTE CELLS OF NECTURUS. D.W.McBride,Jr. S.Roper, Dept. of Anatomy/Neurobiology, Colorado St. Univ., Ft. Collins, CO. 80523, Intr. by T.N. Solie.

Ion channels inevitably play an important role in chemosensory transduction mechanisms. We have investigated the regional localization of ion channels in taste cells. Sheets of lingual epithelium from Necturus maculosus were dissected from the animal and placed in a modified Ussing chamber. This permitted solution isolation between the mucosal and serosal surfaces of the epithelium. Solutions and agents applied to one surface do not diffuse to the opposite side. With our chamber, taste buds were visualized under a water immersion objective at 400X and individual cells impaled with microelectrodes. During an impalement, top and bottom chambers were perfused independently and with several changes. With symmetrical solutions of amphibian physiological saline (APS) (noted APS/APS), action potentials (a.p.) can be elicited by current injection. When 8 mM TEA was added to the mucosal chamber (TEA-APS/APS), the shape of the a.p. was strikingly changed(Fig.1). TEA in the serosal chamber (APS/TEA-APS) produced no significant change in the shape of the a.p. This indicates that K-delayed rectifiers are preferentially located in the apical membrane. A series of substitution experiments (choline for Na^+, Mg^{++} for Ca^{++}) revealed that Na and Ca channels are located on both apical and basolateral membranes. Another series of substitution experiments, (Ba^{++} for Ca^{++} in the presence of TEA) revealed the presence of a Ca-mediated, TEA-insensitive, inward current on the basolateral and not on the apical membrane(Fig.2). Supported by NIH grants NS24107, NS20486, and AG06557.

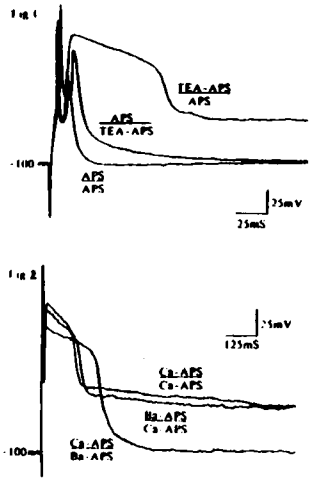

M-AM-B2 NON-UNIFORM DISTRIBUTION OF K^+ CHANNELS SUBSERVES TASTE TRANSDUCTION IN MUDPUPPY. S.C.Kinnamon*, V.E. Dionne+ & K.G. Beam#. Depts. of *Anatomy/Neurobiology & #Physiology, Colorado St. Univ., Ft. Collins, CO 80523; +Dept. of Pharmacology, Univ. of California, San Diego, CA 92093.

Taste transduction must involve an interaction of chemical stimuli with the apical membrane of taste receptor cells, but the mechanisms are poorly understood. Previous studies on isolated mudpuppy taste cells have shown that sour taste stimuli applied to the entire cell reduce a voltage-sensitive K^+ conductance (g_K). If g_K were uniformly distributed, then reducing g_K only in the apical membrane (<5% of total cell membrane), would produce little receptor potential. To map ion channel distribution, we have used a loose patch pipette (3-4 μm tip) to record currents through small patches of membrane in response to voltage commands generated by a second, whole-cell pipette. The apical surface of the lingual epithelium was exposed to FITC-WGA to label the apical membrane of taste cells isolated by subsequent dissociation. K^+ current was evoked by stepping from the holding potential (-100 mV) to +80 mV; Na^+ current was elicited by stepping from -100 to -20 mV. For the cell shown, 10% of the whole-cell K^+ current was recorded from a loose patch near ($\leq$ 5 μm) the apical membrane, whereas only 0.2% was recorded from a loose patch in the basolateral region. For the 19 taste cells mapped, g_K (per unit area) was almost 50-fold greater on the apical membrane than on basolateral membrane, whereas g_{Na} was nearly the same in the two regions. These results support the hypothesized role for g_K in sour taste transduction. Supported by NIH grants NS20382 (SCK), NS20962 (VED) and NS24444 (KGB).

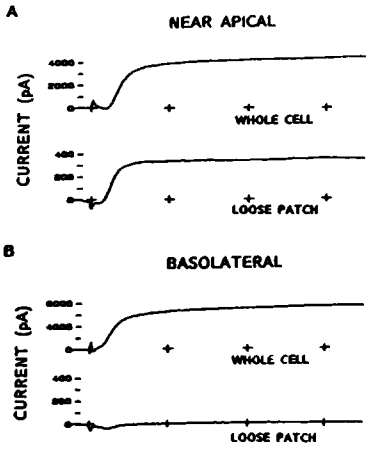

M-AM-B3 THE RETINAL ROD GTPase RATE INCREASES WITH MEMBRANE CONCENTRATION: EVIDENCE FOR A WEAKLY MEMBRANE BOUND CONTROL FACTOR. E.A. Dratz,* D. Siemsen,* J.W. Lewis and D.S. Kliger, *Department of Chemistry, Montana State University, Bozeman, MT 59717; Department of Chemistry, University of California, Santa Cruz, CA 95064.

Guanosine triphosphate (GTP) binding proteins mediate cellular responses to hormones, neurotransmitters, growth factors and light. Activated GTP binding proteins shut off by GTPase mediated hydrolysis of GTP. GTPase rates are reported to be 10-50 times too slow to account for the shutoff rate of the response of the photoreceptor to light stimulus. Recovery rates of other parts of the system appear fast enough, and the GTPase rate appears to be rate limiting for shutoff. The GTPase rate increases linearly with photoreceptor membrane concentration up to an experimental limit of 30 mg/ml. If all relevant components were tightly membrane bound, there would be no change in surface concentration with dilution of the suspension and the turnover rate would be independent of membrane concentration. Therefore, these results imply the existence of a weakly membrane bound factor controlling the GTPase. If extrapolated to physiological concentration (ca. 130 mg/ml), the GTPase turnover is fast enough (1-4 sec^{-1}) to account for the recovery of the light stimulated response of photoreceptor cells. Low affinity binding interactions may be crucial in cellular control mechanisms. Forward control reactions can be no faster than diffusion limited, and if they are also to be rapidly reversible, they cannot involve high affinity binding ($K_{bind} = k_{forward}/k_{reverse}$). (Supported by NIH RO1 EY06915.)

M-AM-B4 BIVALENT LIGAND-SURFACE IMMUNOGLOBULIN DISSOCIATION KINETICS AS A PROBE OF CELL SURFACE DYNAMICS J. Erickson, *B. Goldstein, D. Holowka, B. Baird. Dept. of Chemistry, Cornell University, Ithaca, NY 14853 and *Theoretical Division, Los Alamos National Laboratory, Los Alamos, NM 87545.

Crosslinking of receptor bound immunoglobulin E (IgE) on the surface of mast cells and basophils initiates the cascade of events that results in the secretion of mediators in the allergic response. We have been investigating the first step in this process by focusing on the binding of small, well defined ligands containing (2,4)-dinitrophenyl (DNP) groups to fluorescein labeled, monoclonal anti-DNP IgE (F-IgE). Characterization of the equilibrium binding or association kinetics for monovalent DNP-aminocapryol-L-tyrosine (DCT) or bivalent $(DCT)_2$-cystine has been assessed previously in this lab by monitoring fluorescence quenching of fluorescein by DNP. Conversely, dissociation of ligand is observed as an increase in fluorescence when excess unlabeled anti-DNP IgE is added to a pre-equilibrated mixture of F-IgE and DNP ligand. At nanomolar concentrations of F-IgE free in solution, DCT and $(DCT)_2$-cys dissociation proceeds in a unimolecular fashion yielding a single rate constant, k_{off}=.05/s. However, when F-IgE is bound to its high affinity receptor on the membrane surface, $(DCT)_2$-cys exhibits a much slower, two phase rate of dissociation well fitted by an intrinsic k_{off} similar to that for DCT (also .05/s on cells) and a second dissociation constant characterizing the mean lifetime of the crosslinks (k_{x-}) about 500x smaller than k_{off}. Perhaps most interesting is the dependence on the $(DCT)_2$-cys pre-incubation time for cell bound $(DCT)_2$-cys dissociation curves. This time dependence is not due to receptor internalization and is not observed with RBL cell vesicles which lack an intact cytoskeleton. The possibility that the time dependent loss of dissociability may be correlated with the biological potency of a given ligand-IgE pair is being explored. Supported by NIH grants AI22449-01 and GM35556 (B.G.)

M-AM-B5 SURFACE POTENTIALS OF POLYSTYRENE MICROSPHERES AND THEIR RELATIONSHIP TO NEUTROPHIL STIMULATION. Jerome Cuttitta, Bruce Marlowe and Vincent A. DeBari. Seton Hall Univ., So. Orange, NJ and The Renal Lab., St. Joseph's Hosp. & Med. Ctr., Paterson, NJ (JC & VADB) and Pen-Kem Inc., Bedford Hills, NY (BM).

In previous work (Orsini et al, Cell Biophysics 10, 33-43; 1987) we demonstrated significant differences in the ability of polymorphonuclear neutrophils (PMN) to respond to polystyrene microspheres (PM) of varying surface functionality (underivatized, P; amino, P-NH_2; carboxyl, P-COOH; hydroxyl, P-OH). Using two sets of experimental parameters, those generated from luminol-dependent chemiluminescence and from microscopic observation of phagocytosis, PMN were found to respond in the order: P> P-COOH> P-OH> P-NH_2. Here, we report on our attempts to correlate these data with the surface potentials obtained through particle electrophoresis studies.

Because measurements of particle mobility are strongly dependent on the ionic composition of the milieu, these studies were performed on particles suspended in HEPES-buffered Ringer's, pH 7.4 containing 1 mM $CaCl_2$, i.e., the identical buffer used in the above mentioned studies. Histograms of electrophoretic mobility (μ) demonstrated that the PM were fairly monodisperse with respect to μ. Zeta potentials were calculated from μ and were found to be (mean ± 1 SEM, n=5 for each): $-4.32 \pm 0.204 \times 10^{-2}$ mv (P), $-4.31 \pm 0.021 \times 10^{-2}$ mv (P-COOH), $-3.38 \pm 0.033 \times 10^{-2}$ mv (P-OH) and $-2.97 \pm 0.142 \times 10^{-2}$ mv (P-NH_2). These data suggest that prediction of neutrophil stimulation in this system cannot be made purely on the basis of zeta potential. Other possible models may require a knowledge of the particle surface charge density and/or the thickness of the electrical double layer.

M-AM-B6 LIGAND-RECEPTOR AND RECEPTOR-G PROTEIN DYNAMICS IN THE NEUTROPHIL. L.A. Sklar, W. Swann, G. Bokoch. Dept. Imm., Res. Instit. of Scripps Clinic, and H. Motulsky, Dept. of Pharmacology, UCSD, La Jolla, CA.

Neutrophils, the most numerous of the white blood cells in man, participate in inflammation and host defense. Their chemotactic and inflammatory responses are triggered by the binding of ligands (L) to cell surface receptors (R). Signal transduction involves guanine nucleotide binding protein (G). To examine the dynamics of the interactions among L, R, and G we have employed permeabilized cells, a fluorescent ligand for the formyl peptide receptor (N-formyl-Nle-Leu-Phe-Nle-Tyr-Lys-fluorescein) and a combination of real-time spectroscopic methods which are capable of resolving interactions between ligand and receptor over concentrations ranging from pM to uM. In the absence of guanine nucleotide, the association of L and R to form a slowly dissociating ($t_{½}$~100 sec) ternary complex LRG appears to be a single step proceeding at a rate ($3x10^7$/Msec at 37°) which approaches the 3D diffusion limit. Such single step kinetics can arise either because 1) RG is precoupled (and binding of L is formally single step) or 2) because the interaction between R and G occurs in <sec in 2D following the binding of L to R and there is sufficient G to accommodate all the LR as it forms. In the presence of guanine nucleotide or when R and G are uncoupled by ribosylation or alkylation of G, the binding of L to R exhibits the same association rate, but rapid dissociation ($t_{½}$~10 sec). The guanine nucleotide dependent dissolution of LRG into LR+G occurs at a rate proprotional to guanine nucleotide concentration. At physiologic nucleotide concentration, this interconversion - which mimics the activation of G - should occur in<sec. Thus the two steps in transduction, formation of LRG and activation of G are rapid.

M-AM-B7 **Dimerization kinetics of the IgE-class antibodies and divalent haptens**

R. Schweitzer-Stenner[1], A. Licht[2], and I. Pecht[2]
1. University of Bremen, FB 1 - Physik, 2800 Bremen 33, F.R.G.
2. Weizmann Institute of Science, Dept. of Immunology, Rehovot, Israel.

The oligomerization of monoclonal DNP specific IgE-antibodies into open and closed dimers which occurs upon binding of divalent haptens (SCHWEITZER-STENNER et al., Biochemistry 26, 3062, 1987) proceeds slowly at 37° C. To investigate the kinetic processes, we performed fluorescence titrations of divalent DNP-haptens with different spacer length (14 Å - 130 Å) to both, monomeric Fab-fragments and intact IgE's. Changes in the hapten addition rate causes significant variations of the titration curves. These were analysed by inserting a kinetic model into the theory of DEMBO and GOLDSTEIN (J. Immunol. 121, 345, 1978). The application of this theory into a fitting procedure for the titrations yields the following results: 1) Haptens with short and flexible spacers cause a relatively slow dimerization of both, the Fab-fragments and intact IgE's. For instance association and dissociation constants have been calculated to be 1.75×10^5 M^{-1} sec^{-1} and 1.3×10^{-2} sec^{-1} for bis (DNP-ß-Ala)-diamino succinate, respectively. 2) In contrast to this, large and rigid oligoproline haptens (bis (DNP)-Ahx-Asp-$(Pro)_n$-Lys, n = 24,27,33,37) cause a comparatively fast dimerization of the Fab-fragments. The kinetic parameters of the respective reactions with intact IgE's strongly depend on the length of the oligoproline spaces. For the long haptens (130 Å) a rather slow component of the oligomerization process could be obtained (10 sec). This is probably due to the ring closure process (BARISAS et al., Immunochemistry, 14, 247, 1972).

M-AM-C1 STEADY STATE SLOW INACTIVATION OF SODIUM CHANNEL GATING CURRENTS. W. J. Adelman, Jr.[1] and J. F. Fohlmeister[2], Lab. Biophys. (1) NINCDS, NIH, Bethesda, MD 20892, and Lab. Neurophysiol.(2) U. Minn., Minneapolis, MN 55455

Gating current or asymmetry current is a component of the dielectric displacement current that is correlated with activation gating of the voltage-sensitive sodium channels. Gating currents are assumed to be the reasonably direct external expression of certain conformational changes within the channel molecule or of realignments among channel subunits. This study investigated the question of whether long duration voltage conditioning produces measureable changes in the gating current and whether these are related to slow sodium inactivation.

Squid giant axons, perfused with Na and K free Cs solution internally and with Tris-TTX sea water externally, were sinusoidally voltage clamped following a long duration (up to several minutes) conditioning D.C. voltage. Harmonic analysis of the sinusoidal asymmetry currents showed that these currents were significantly altered by both hyperpolarizing and depolarizing long duration voltages. These effects were eliminated by internal perfusion with pronase. The effects were shown to be related to the slow inactivation of sodium channel ionic currents.

M-AM-C2 OPEN SODIUM CHANNELS INACTIVATE WITH A VOLATGE-INDEPENDENT RATE CONSTANT IN PITUITARY CELLS. Clay M. Armstrong and Gabriel Cota*, Dept. of Physiology, University of Pennsylvania, Philadelphia, PA 19104 and *Dept. of Physiology, CINVESTAV-IPN, Mexico, DF.

Intracellular papain removes Na channel inactivation in neuroblastoma cells (Gonoi & Hille 1987, J.G.P. 89:253). We studied papain action in GH3 cells, and determined the rate constant of the inactivation step by comparing I_{Na} traces before and after the removal of inactivation. We used patch pipettes to record whole-cell currents and to apply papain internally. Voltage-clamp speed was increased by 'supercharging'. Na channels were opened by a brief activating pulse to +60 mV. Voltage was then stepped to a new level to examine closing kinetics. Channels can close by inactivating, or by deactivating (i.e., by closure of either the inactivation or the activation gate). With inactivation intact, closing is exponential with a rate that is the sum of the inactivation and the deactivation rate. Closing rate decreases on lowering the repolarization level from -100 to -20 mV. From -20 to +60 mV the closing rate has a fixed value of about 1.5 ms^{-1} at 15°C. After removal of inactivation channels no longer close for voltages positive to -20 mV. Thus closing of unmodified channels at these voltages results from inactivation, at a rate that is not dependent on voltage. Negative to -20 mV, kinetics are complicated by a spontaneous left shift of gating parameters, not related to papain. Taking this into the analysis, we find that inactivation rate is voltage-independent from -100 to +60 mV.

M-AM-C3 ION CHANNEL SELECTIVITY IS RELATED TO GATING KINETICS. Martin Blank, Department of Physiology and Cellular Biophysics, Columbia University, 630 West 168 Street, New York, NY 10032.

It has been possible to describe ionic processes in the electrical double layers at membrane surfaces during current flow using the Surface Compartment Model (BBA 906,227-294, 1987). The SCM has been applied to a voltage gated channel whose conductance varies with the charge density at the inner surface, as suggested by an oligomer disaggregation model for channel opening (Bioelectrochem. Bioenerg. 9,615-624, 1982). When using parameters that are appropriate for the squid axon membrane it has been found that the ionic flow through a channel depends upon the gating current (i.e., the speed with which it opens). With equivalent depolarization, a fast gating channel shows an inward sodium current and a slow gating channel shows an outward potassium current. The apparent selectivity, which depends upon the electrochemical gradients at the time of opening, varies because of the difference between the rapid change in electrical potential and the slower changes in the ionic concentrations (i.e., chemical potentials) that result from the electrical transference and the charging of the membrane capacitances when the voltage clamp is imposed. Ionic concentration changes due to transference are considerable in membrane systems having large gradients initially (J. Electrochem. Soc. 134,1112-1117, 1987) and should be taken into account when interpreting measurements made under imposed polarizations.

(Supported in part by ARO contract DAAL03-86-K-0162.

M-AM-C4 **SIALIC ACID-SPECIFIC LECTIN AFFINITY RESIN FOR PURIFICATION AND RECONSTITUTION OF THE ELECTROPLAX Na CHANNEL** W.M. James & W.S.Agnew, Cellular and Molecular Physiology, Yale Univ. Sch. Med., New Haven, CT 06510.

The voltage-sensitive Na channel from eel electroplax is a large glycopeptide bearing ~85 kDa of carbohydrate, including extended, unbranched homopolymers of 2,8-linked polysialic acid. Seven lectins were surveyed for application as affinity reagents, including three that interact with sialic acids, agglutinins from wheat germ, Limulus polyphemus and from Limax flavus (LFA). LFA coupled to CNBr activated Sepharose was found to avidly adsorb the ^{3}H-TTX binding Na channel. The protein could be desorbed with NeuNAc, ($K_{1/2}$~ 0.4 mM). When mixed with protein previously purified by one step of DEAE Sephadex anion exchange chromatography, ^{3}H-TTX binding sites were adsorbed in a biphasic time course requiring ~90 min for >95% uptake. Protein failed to desorb with extended washing but could be eluted (>90%) within 2 minutes after addition of 10 mM NeuNAc. This affinity resin served in a two step purification (ion exchange and lectin affinity chromatography) that yielded purity comparable to that previously achieved with ion exchange followed by one step of gel filtration chromatography. Because the procedure is rapid (less than 5 hours), resulting in minimal denaturation, the protein can be purified without addition of stabilizing neurotoxins, an advantage for functional reconstitution studies. For optimizing reconstitution, the protein could be concentrated to high levels without concomittant concentration of lipid and detergent. Resin containing 5 mg LFA/ml, with capacity 0.3 mg protein/ml, packed into a column of 0.3 x 47 cm, eluted step-wise with 10 mM NeuNAc yielded protein at 1.25 mg/ml in 0.1% Lubrol- PX:Phosphatidylcholine (7:1) buffer. Dilution to desired levels in lipid suspensions, followed by reconstitution and fusion into large liposomes resulted in highly active Na channels in radio- tracer flux assays and patch-clamp recording studies. (Supported by NIH NS 17928 to WSA)

M-AM-C5 PURIFICATION AND CHARACTERIZATION OF TWO SODIUM CHANNELS FROM RAT BRAIN WITH DIFFERENT ALPHA SUBUNITS AND DISTINCT FUNCTIONAL PROPERTIES. Adrian M. Corbett and Bruce K. Krueger, Dept. of Physiology, Univ. Maryland School of Medicine, Baltimore, Maryland 21201.

Voltage-dependent Na channels have been purified from electric eel electroplax, rat brain, and rat and rabbit skeletal muscle transverse tubules using binding of radiolabeled saxitoxin (STX) or other neurotoxins to assay for the channel protein. Each Na channel consists of a single large alpha subunit (M.W. about 260K) and, except for the electric eel, one or two beta subunits (M.W. about 35 - 39K). Using a modification of the procedure described by Hartshorne and Catterall (J.B.C. 259: 1667, 1984) and HPLC in the final steps to improve resolution, we separated two ^{3}H-STX binding proteins with different alpha subunits (M.W. 235K and 265K) as revealed by SDS-PAGE. Both channel types had similar beta subunits. These channels were reconstituted in planar lipid bilayers for characterization of channel function. In the presence of veratridine (VER), the Na channel with the 235K alpha subunit had a conductance of 10 pS and resembled that described by Garber and Miller (J.G.P. 89: 459, 1987). Extracellular scorpion venom (Leiurus quinquestriatus) caused a small (15%) increase in single channel conductance and an increase in the probability of being open. In contrast, the Na channel with the 265K alpha subunit had a conductance of 5 pS in the presence of VER and underwent about an 80% increase in single channel conductance in the presence of scorpion venom (to 9 pS) together with an increase in the probability of being open. Both 10 pS (M.W. 235K) and 5 pS (M.W. 265K) Na channels displayed voltage-dependent gating and were blocked by nanomolar concentrations of STX. Supported by NIH.

M-AM-C6 DIFFERENTIAL EXPRESSION OF Na CHANNEL SUBTYPES IN TWO POPULATIONS OF SENSORY NEURONS. Donald T. Campbell, College of Pharmacy and Hatfield Marine Science Center, Oregon State University, Newport, OR 97365.

Single dorsal root ganglion cells from garter snakes were enzymatically dissociated. Na currents were measured using the whole-cell voltage clamp technique. Test solutions contained (mM) 120 NaCl, 20 TEACl, 10 CsCl, 5 HEPES (pH 7.4) 1 $CaCl_2$, 9 $MgCl_2$. $LaCl_3$ (10 uM) was present to block calcium currents. Replacement of Na by TEA caused the early transient current to become outward, suggesting that it is carried by Na channels. Cell capacitance ranged from 4 to 34 pF. The largest cells (capacitances >23 pF) all exhibited block by TTX appropriate for a single class of Na channels with a K_d of 40-50 nM (n=9). In 17 of 19 smaller cells (capacitance < 20 pF; mean 11.2 pF) 2 kinds of Na channels were present: 1) channels with a sensitivity to TTX similar to that of the larger cells; and 2) a second population nearly totally resistant to block by TTX. In this group of cells, 1 or 5 uM TTX left 31 ± 21% of the Na current unblocked. In 2 of the cells, 1 uM TTX blocked >94% of the Na current. The TTX-resistant current reverses at the same potential as the TTX-sensitive current, but inactivates more slowly. The resistant current was little affected by TTX concentrations up to 100 uM. 1 uM STX blocked virtually all of the TTX-sensitive Na current without reducing the TTX-resistant current. STX-resistance distinguishes these TTX-resistant channels from the resistant channels found in frog sympathetic ganglia (S.W. Jones, 1987, J. Physiol. 389: 605). Supported by NS 22577 and MDA.

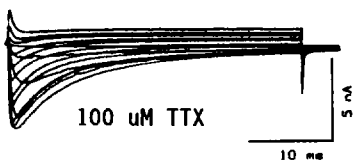

M-AM-C7 Na CURRENT RELAXATION TIMES IN SQUID AXON: HH TRANSIENT ANALYSIS YIELDS DIFFERENT RESULTS FROM LINEAR STEADY-STATE ANALYSIS. H.M. Fishman and H.R. Leuchtag, University of Texas Medical Branch, Galveston, Texas and Texas Southern University, Houston, Texas.

Application of the Hodgkin-Huxley (HH) formulation and methodology has become standard procedure for obtaining quantitative estimates of the linear macrokinetic relaxation times τ_m and τ_h in Na and other ion conducting preparations that exhibit activation and inactivation processes. In light of our previous finding that an HH kinetic analysis of K current relaxations does not yield the relaxation time (τ_p) of the linearized conducting system (B.J. 51:51a:1987), we examined the analogous question for the Na conductance process in squid axon. Fits of the equation $I_{Na} = I_o(1 - Ae^{-t/\tau_m})^x (1-Be^{-t/\tau_h})^y$ to Na current responses in squid axons, internally perfused with buffered solutions containing 200 mM Cs, 100 mM K and 150 µM 3,4 DAP, for voltage clamp steps of 30 to 90 mV from a holding potential of -75 mV, yielded significantly better fits (least-squares criterion) when the exponents x and y were allowed to vary than when they were fixed at the HH values of 3 and 1. Direct linear analysis by measurement of membrane admittance under the same conditions and in the same axon in the steady state (100-200 msec after step clamps) and curve fit of the admittance at each clamp voltage by the equation $Y(j\omega) = [R_s + (Y_m)^{-1}]^{-1}$, where $Y_m = (j\omega)^\alpha C_m + g_o + g_m(1 + j\omega\tau_m)^{-1} + g_h(1 + j\omega\tau_h)^{-1}$ in the frequency range 2.5 to 5000 Hz yielded estimates of $\tau_m(v)$ and $\tau_h(v)$ that differ from the estimates obtained by HH analysis. We conclude that either (1) Na conductance kinetic parameters change with time or (2) an HH analysis is not equivalent to a linear analysis and yields values of τ_m and τ_h that are purely empirical. Supported by NIH grant NS11764 and ONR Contract NOOO14-87-K-0055.

M-AM-C8 **Chloroform and the birefringence response of the squid giant axon.**

David Landowne Department of Physiology and Biophysics • University of Miami School of Medicine • Miami,FL 33101

Segments of squid axons were internally perfused and voltage-clamped with an axial internal electrode assembly. A beam of plane polarized light from a tungsten-halogen bulb passed through the preparation from below at 45° with respect to the axis. A second polarizer perpendicular to the first was mounted above the nerve and a photodetector placed above this analyzer. The birefringence response is seen as a change in light level at the detector associated with a change in nerve membrane potential. The pulses were symmetrical, ±80 mV for 4 msec from a -80 mV holding potential.

By the end of the depolarizing pulse the birefringence had decreased by 29 ± 5 (n=6) parts per million; during the hyperpolarization the birefringence increased by 41 ± 6 ppm. Repeat measurements were 1.02 ± .04 and 1.07 ± .14 of the first trial. When 62 mM chloroform (v/v) was included in the internal perfusion fluid these amplitudes were reduced by about 20% to 21 ± 3 and 33 ± 6 ppm ($p < .05$, paired t-test). Concomitantly the ionic sodium current was reduced by more than 90%. On washout, recovery of the optical signal was poor and often contaminated by the rise of the secondary biregringence response. Measurements at 300 µsec have less statistical significance but suggest the same story.

Fernandez, Bezanilla and Taylor (*Nature* **297**:150-2) reported this concentration of chloroform reduced a rapid component of the gating current by about half or the total charge movement by about 20% (Cf. *Biophys.J.* **23**:479-84). Thus there is similarity between the effects of chloroform on the birefringence response and on the polarization currents.

This work was supported by a grant from the Whitehall Foundation and NSF grant BNS-8514312.

M-AM-C9 *SIGNAL CONDUCTION AND IONIC CHANNELS IN SINGLE REMYELINATING AXONS.*

Peter Shrager, Department of Physiology, University of Rochester Medical Center, Rochester, NY 14642

When demyelinated axons are remyelinated new nodes of Ranvier are formed in regions that were previously internodal. The distribution of Na^+ and K^+ channels has been studied in single frog sciatic fibers as new myelin develops. Axons were examined with the loose patch clamp up to 5 months following acute focal demyelination induced by intraneural injection of lysolecithin. It has previously been shown that Na^+ channels are present in the internodal axolemma as early as 1 day post injection (P.I.). Peak inward internodal currents are constant from 1 week to 6 weeks P.I., but then increase by about 60% over the next 4 months. New nodes of Ranvier, on the other hand, have significantly larger currents, with patches producing 3 to 4 times the inward current of internodal regions. Schwann cells, proliferating in the demyelinated zone at 3-6 weeks P.I have no significant Na^+ current as measured with the loose patch clamp. Nodes of Ranvier marking the transition from old to new myelin can be identified at all stages. Paranodal records at these sites show that over a limited range of depolarizations inward currents are abruptly terminated by a large transient outward current. This pattern is likely to result from a very high density of Na^+ channels located just outside the patched zone. This region 'escapes' potential control and Na^+ currents return as outward current through the pipette. The above result is not found at internodal sites nor is it seen at new nodes. However, it persists at transition nodes up to 21 weeks P.I. Thus, if lateral diffusion of Na^+ channels into the demyelinated internode occurs it may involve only a small fraction of the nodal channels. With a patch held at the resting potential, the nerve can be stimulated externally several mm proximal to the lesion. At 2-3 weeks P.I. conduction is severely compromised just 200 µm beyond the proximal border of intact myelin. Responses have been recorded from axons at the distal end of the lesion but thus far only small outward currents have been seen despite the presence of Na^+ channels. At this stage there is a population of fibers with a very low conduction velocity. It remains to be seen whether this represents 'continuous' conduction or results from early limited remyelination. Supported by grants from the NIH (NS-17965) and the NMSS (RG-1774).

M-AM-C10 **CHARACTERIZATION OF A REGION IN THE RAT TYPE II SODIUM CHANNEL GENE THAT CONFERS CELL SPECIFIC EXPRESSION** R.A. Maue, S. Cooperman, M. Begley, R.H.Goodman, and G. Mandel
Division of Molecular Medicine, New England Medical Center, Boston, MA 02111

The functional significance of multiple Na channel genes is not clearly understood. It is possible the genes encode functionally different ion channels or are subject to different regulatory influences. In previous studies we examined the regulation of the rat type II Na channel gene by nerve growth factor and the functional properties of the type II gene in PC12 cells (Cooperman et al., PNAS , in press). More recently, we have begun to identify the sequences in the type II Na channel gene that are required for expression in PC12 cells and other excitable cells. Synthetic oligonucleotides complementary to sequences in the 5' untranslated region of the rat brain type II Na channel cDNA were used to screen a rat genomic DNA library and isolate a large DNA fragment. Restriction mapping and Southern blot analysis identified a segment corresponding to 1.1 kb of the 5' flanking region. A fusion gene was constructed containing this 5' flanking region linked to the prokaryotic reporter gene chloramphenicol acetyltransferase (CAT). The expression of this construct (pMB2) was examined in cells transfected with 20 ug of pMB2 using either electroporation or calcium phosphate coprecipitation. Cells were harvested 48 hours after transfection and cell extracts were assayed for CAT activity.To control for variations in transfection efficiency, expression of pMB2 was normalized to the expression of RSV-CAT (CAT expression under the control of the Rous sarcoma virus promoter and enhancer) and pSV2-CAT (CAT expression under control of the Simian virus 40 early promoter and enhancer). The normalized level of expression of pMB2 was 5 to 50 times higher in electrically excitable cells, such as rat pheochromocytoma (PC12), mouse anterior pituitary (ATT20), and human neuroblastoma cells (NB-5), than in a variety of inexcitable cells, including rat glioma (C6), rat myoblasts (L6), mouse fibroblasts (NIH 3T3), mouse myoblasts (C2), and human cervical epithelial cells (Hela). To determine the boundaries of the sequences required for cell specific expression, deletions were made from the 5' end of the Na channel DNA insert in pMB2. A fusion gene containing only 350 bases of the Na channel DNA expresses equally well as pMB2 in the excitable cell types and exhibits the same pattern of cell specific expression.The results of these studies will be important in identifying elements responsible for determining electrical excitability. In addition , because the voltage-dependent Na channel is often fundamental in determining the neuronal phenotype, understanding the mechanisms controlling expression in this gene family will provide insight into general mechanisms of neuronal development and differentiation. Supported by NS22518 and IF32NS07884 to G.M. and R.A.M.

M-AM-C11 **CHANGES IN HOLDING POTENTIAL DEMONSTRATE A SYMMETRICAL STEADY STATE CHARGE DISTRIBUTION IN CRAYFISH AXONS.** J.G. Starkus and M.D. Rayner
Bekesy Lab. of Neurobiology and Dept. of Physiology, U. of Hawaii, Honolulu, HI. 96822

Changes in holding potential from -140 to -70 mV result in suppression of ON gating current observed at 0 mV test potential and increase in OFF gating current at -240 mV. Both Q ON and Q OFF can be plotted as a function of holding potential, providing two potentially alternative measures of steady state charge distribution. In our data these two curves (obtained using 0 mV and -240 mV test potentials) are symmetrical and overlie if inverted. The midpoint of this distribution is about -100 mV, while the slope of the steady state curves indicates an effective particle valence of about 1.8e. The total charge moved (the sum of Q ON and Q OFF) is typically between 35 and 40 nC/cm2 at all holding potentials.

The Q ON curve obtained is not markedly altered when the conditioning potential and P/n pulses for subtraction of linear capacity currents are shifted from a negative voltage range to positive potentials. We conclude that little charge moves in the voltage range used for negative P/n pulses, even when depolarized holding potentials are used. Our results do not seem consistent with the simplified 4-state model introduced by Bezanilla et al. (JGP 79:41-67, 1982) and tested in the frequency domain by Fernandez et al. (JGP 79:21-40, 1982). By contrast these data are fully consistent with the 8-state model presented by Bezanilla et al. (JGP 79:41-67, 1982).

Supported by PHS grant #NS21151-04, Hawaii Heart Association, and UHBRSG.

M-AM-C12 **HOLDING POTENTIAL AFFECTS THE SHAPE OF THE Q-V CURVE IN CRAYFISH GIANT AXONS.** M.D. Rayner and J.G. Starkus
Dept. of Physiology and Bekesy Lab. of Neurobiology, University of Hawaii, Honolulu, HI.

From a holding potential (Vh) of -140 mV, the Q-V curve is a simple sigmoid suggesting an effective particle valence of 1.8e and Qmax of 35 to 40nC/cm2. At Vh = -100 mV the curve divides into two equal parts: a "low slope" region (0.8e) extending from Vh to -240 mV and a "high slope" region (1.8e) between -80 and 0 mV. The fraction of total charge associated with the low slope region increases as Vh is further depolarized, reaching 0.95 at Vh = -70 mV in these axons. Qmax, assessed as the maximum ON plus OFF charge movement, is not affected by change of Vh.

We find that, at any Vh, there is an asymmetry in the membrane's response to depolarizing and hyperpolarizing test pulses. For depolarizing test pulses, voltage sensitive charge movement is complete in less than 4 ms. By contrast for hyperpolarizing test pulses, voltage sensitive charge movement may continue for more than 100 ms. Hence the "low slope" region of the Q-V curve (demonstrated in hyperpolarizing test pulses from Vh) reflects incomplete voltage sensitive charge movement rather than a reduced effective gating particle valence.

Our data are in quantitative accord with the predictions of the 8-state model proposed by Bezanilla et al (JGP 79:21-40, 1982), after adjusting for differences between squid and crayfish gating current kinetics and steady state voltage sensitivities.

Supported by PHS grant #NS21151-04, Hawaii Heart Association, and UHBRSG.

M-AM-D1 **EXPRESSION OF THREE CALCIUM CHANNEL SUB-TYPES OCCURS SEQUENTIALLY IN DEVELOPING SKELETAL MUSCLE CELLS AND IS BLOCKED BY TRANSFORMING GROWTH FACTOR β (TGFβ), AN INHIBITOR OF MYOGENIC DIFFERENTIATION.** J.M. Caffrey*, A.M. Brown*, and M.D. Schneider*+. Depts. of *Physiology & Molecular Biophysics, +Medicine, and +Cell Biology, Baylor College of Medicine, Houston, Texas.

Formation of functional "fast" and "slow" Ca^{2+} channels in BC_3H1 myoblasts requires mitogen withdrawal and can be blocked by an activated ras allele which prevents myogenic differentiation (Science 236:570). Whether single peptides that inhibit myogenesis can control Ca^{2+} channel expression is unknown. We have analyzed the ontogeny of Ca^{2+} channels in C2 muscle cells following mitogen withdrawal at sub-confluent density (V_h = -90mV): (i) No Ca^{2+} channels were expressed in proliferating myoblasts. (ii) Functional "transient" Ca^{2+} channels were expressed within 24 hours of mitogen withdrawal, 1 to 2 days before appearance of "fast" and "slow" channels. (iii) All three components of current coexisted in biochemically differentiated, unfused cells after 3-4 days. (iv) "Transient" channels subsequently were deinduced; only "fast" and "slow" channels were expressed following mitogen withdrawal for 14 days. (v) Formation of all three components of Ca^{2+} current was suppressed reversibly by 1 nM TGFβ. Thus, expression of Ca^{2+} channel sub-types occurs sequentially during myogenesis and can be regulated by TGFβ, a peptide which prevents the activation of muscle-specific genes.

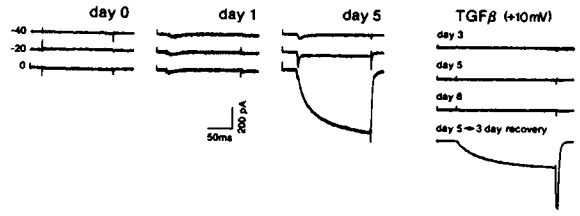

M-AM-D2 CALCIUM-DEPENDENT POTENTIATION OF HIGH THRESHOLD CALCIUM CHANNELS DURING REPETITIVE DEPOLARIZATION IN GUINEA PIG VENTRICULAR MYOCYTES. Andrew C. Zygmunt, Dept. of Physiol.; and James Maylie, OB Research, Oregon Health Sciences University, Portland, OR 97201.

We have measured a frequency-dependent depotentiation of low threshold T-type calcium channels (25-40% at -30 mV), and a potentiation of high threshold L-type channels (20-40% at 30 mV), as reported by Mitra and Morad (1986) and Lee (1987). L-type channel potentiation was associated with a delay in onset of inactivation. The rate of rise and the steady state current levels were unchanged with potentiation. This potentiation was calcium-dependent, since barium as the charge carrier resulted in loss of potentiation (T-type channels were unaffected). T-type channel activation by dual pulses to -30 mV or its inactivation by 500 ms prepulses to -40 mV failed to modulate the potentiation of the L-type channels. In dual pulse protocols to 30 mV, shortening of the first pulse to 10 ms elicited a potentiation equal to that with a 150 ms first pulse. In experiments in which the interpulse interval between two test pulses to 20 mV was increased 10-200 ms, the P2/P1 ratio of peak currents increased from 0.2-1.4. This ratio slowly decreased with a half-time of 4 seconds as the interpulse duration was further increased. The calcium agonist BAY K 8644 (5.0 uM) increased L-type channel currents 2 to 3 fold (T-type channel currents were unaffected) and slightly reduced the degree of potentiation. These data suggest that frequency-dependent potentiation is not dependent upon switching of L-type channels to mode 2 (Hess et al., 1984). The most likely mechanism involves calcium binding to the L-type channel, or calcium activation of some enzyme cascade. T-type channel calcium influx is either insufficient or too distant from the site of calcium-activated potentiation to trigger potentiation.

M-AM-D3 RAPID BLOCK OF CARDIAC CALCIUM CHANNELS AND TENSION DEVELOPMENT INDUCED BY PHOTORELEASE OF EXTRACELLULAR Ca^{2+} IN FROG HEART. M. Naebauer, G. Ellis-Davies, J.H. Kaplan and M. Morad. Dept. of Physiology, University of Pennsylvania, Philadelphia, PA 19104.

Cardiac, skeletal and neuronal Ca^{2+}-channels have been shown to conduct Na^+ when $[Ca^{2+}]_o$ is reduced to about 1uM. In voltage clamped frog ventricular strips, reduction of extracellular Ca^{2+} to 1 uM led to a prolongation of the action potential (20-30 sec duration) which was caused by activation of a TTX-insensitive inward Na^+ current, blocked by Ca^{2+}-channel blockers. The kinetics of the block of this current by extracellular Ca^{2+} were investigated using a newly synthesized photolabile tetracarboxylate Ca^{2+}-chelator, DM-nitrophen, which allowed a stepwise increase in Ca^{2+} concentration (50-100 uM, measured by Ca^{2+} selective microelectrodes) by application of a short UV light pulse (150 us duration). Following photorelease of Ca^{2+}, Na^+ current flowing through the Ca^{2+} channel, irrespective of its direction, was blocked within 500 us, indicating that release of Ca^{2+} from the chelator proceeded even faster. Block of the inward current was accompanied by marked shortening of the action potential. When photorelease of Ca^{2+} reached 30uM levels, significant tension could be measured with 50-100 ms delays in the onset. The potentiation of tension induced by photorelease of Ca^{2+} had a bell-shaped voltage dependence reflecting the voltage dependence of i_{Ca}. The finding that photorelease was more effective in activating tension at the beginning of depolarization compared to 2-3 s into the pulse was consistent with photoreleased Ca^{2+} entering via the inactivating Ca^{2+} channels. We found that Na^+ current through Ca^{2+} channels was blocked within 500 us by Ca^{2+}_o and sufficient Ca^{2+} entered the myoplasm through Ca^{2+} channels to activate tension within 50 ms.

M-AM-D4 IDENTIFICATION OF DRUG RECEPTORS IN Ca^{2+} CHANNEL PREPARATIONS. Pal L. Vaghy, Kiyoshi Itagaki, Edward McKenna and Arnold Schwartz. Department of Pharmacology and Cell Biophysics, University of Cincinnati College of Medicine, Cincinnati, OH 45267.

1,4-dihydropyridine-sensitive, skeletal muscle voltage dependent calcium channels possess two large molecular weight subunits, α_1 and α_2. From these only one, the α_1 subunit binds 1,4-dihydropyridine (DHP) and phenylalkylamine calcium channel inhibitors. This was proven by photoaffinity labeling experiments. The α_1 subunit was weakly stained with silver and revealed an apparent molecular weight of 160-170 kDa on SDS-polyacrylamide gels under both nonreducing and disulfide reducing conditions. The α_2 is heavily stained with silver and its apparent M_r on SDS-polyacrylamide gel was 155-170 kDa under nonreducing and 130-150 kDa under disulfide reducing conditions. The α_1 subunit was phosphorylated with endogenous and exogenous protein kinases but the α_2 was not. Texas red isothiocyanate-labeled concanavalin A, a glycoprotein stain, stained the α_2 subunit but did not stain α_1. Antibodies raised against the α_1 subunit did not recognize α_2 and vice versa. The amino-terminal amino acid sequence of α_1 (MEPSSP) is different from the amino-terminal amino acid sequence of α_2 (EPFPSA). While the α_1 subunit contains several hydrophobic domains which may represent transmembrane segments of this polypeptide, the α_2 is primarily a hydrophilic polypeptide. These data suggest that the α_1 subunit, which is the receptor for DHP and phenylalkylamine Ca^{2+} channel inhibitors, is different from the α_2 subunit which does not bind these drugs. (Supported by NIH grant PO1 HL22619).

M-AM-D5 THE EFFECT OF INACTIVATION OF CALCIUM CHANNELS BY INTRACELLULAR Ca^{2+} IONS IN THE BURSTING PANCREATIC β-CELLS. Teresa Ree Chay, Department of Biological Sciences, University of Pittsburgh, Pittsburgh, PA 15260

Based on recently determined ionic channel properties (Rorsman and Trube, 1985), a simple theoretical model for the burst activity of pancreatic β-cells is formulated. The model assumed that the m gate of an inward voltage-activated Ca^{2+} current is voltage activated and the h-gate is inhibited by intracellular $[Ca^{2+}]$. The probability of opening of the channel gates is represented by Boltzmann equations. In the model, a Ca^{2+} binding site is assumed to exist in the inner membrane of the voltage-gated Ca^{2+} channel. The model predicts that spike and burst electrical pattern can be generated by varying K_h, the binding constant of intracellular Ca^{2+} ions. In addition, varying this parameter results in different levels of intracellular Ca^{2+}. This work was supported by NIH RO1 HL33905-02 and NSF PCM82 15583.

M-AM-D6 REDUCTION OF THE HCO_3/CO_2 BUFFER DECREASES THE FREQUENCY OF GLUCOSE-EVOKED BURSTING IN MOUSE PANCREATIC B-CELLS WITHOUT AFFECTING THE % ACTIVITY: AN EFFECT PREDICTED THROUGH AN INCREASE IN CALCIUM BUFFERING CAPACITY BY THE CHAY-KEIZER MATHEMATICAL MODEL. R. Ferrer, P. B. Carroll, A. C. Boschero, I. Atwater. LCBG, NIDDK, NIH, Bethesda, MD. 20892.

The normal glucose-evoked B-cell electrical activity which correlates closely with insulin secretion, occurs in a spontaneous regular pattern of bursts. The burst period is variable between islets and independent of % activity(%AP). The Chay-Keizer model predicts that a variable burst frequency can be reproduced by altering "f", the ratio of free to total intracellular calcium (Atwater,Rinzel,Plenum 86). As the calcium buffering capacity increases, burst period would lengthen. We reproduced this effect experimentally by altering HCO_3/CO_2. B-cell membrane potentials were measured in microdissected mouse islets perifused with a saline solution containing glucose(11mM), HCO_3(25mM), pH 7.4 equilibrated with 95% O_2 5% CO_2(STD) or with glucose(11mM), Hepes(20mM) pH 7.4 and either HCO_3(5mM added), 100 % O_2 or HCO_3(2.5mM) Air(LOW). LOW solutions slowed the burst frequency from 4.65 ± 0.25/min STD to 2.48 ± 0.18/min LOW ($p<.001$)(n=21). The % AP was not altered significantly: 36.5 ± 2.72 % STD vs 43.7 ± 3.51% LOW. Also, the net uptake of $^{45}Ca^{++}$(pmol/islet/90min) in rat islets was not significantly altered between 4.05 ± 0.32 STD (n=15) and 3.28 ± 0.37 LOW (n=12) (NS) in glucose (0mM) or between 7.25 ± 0.32 STD (n=10) and 6.63 ± 0.45 LOW (n=14) (NS) in glucose(16.7mM). These results may provide insight into abnormalities in ob/ob islets which also have a slow burst frequency.

M-AM-D7 THE G PROTEIN, G_S, DIRECTLY ACTIVATES SKELETAL MUSCLE CA^{2+} CHANNELS. A. Yatani (1), Y. Imoto (1), J. Codina (2), L. Birnbaumer (2), and A.M. Brown (1). Departments of Physiology and Molecular Biophysics (1), and Cell Biology (2), Baylor College of Medicine, One Baylor Plaza, Houston, Tx. 77030.

G-proteins couple various receptors to Ca^{2+} channels. Whether the linkage is only indirect via cytoplasmic second messengers such as protein kinase A (PKA) and protein kinase C (PKC) or is direct, as in the case of the G_{2+}protein G_k and K^+ channels, is unknown. We tested for the latter possibility by recording from Ca^{2+} channels of skeletal muscle T tubule vesicles incorporated into planar lipid bilayers. The cis or cytoplasmic side of membrane was exposed to an ATP-free minimal solution in mM of 50 Na^+(out)/ 50 Na^+, 100 Ba^{2+}, 2 Mg^{2+} (in). Results: (1) Cis, but not trans GTPγS increased single Ca^{2+} channel currents and prolonged open times without affecting unitary conductance. (2) Cis but not trans application of a highly purified G protein (G_s) from human red blood cells, preactivated with GTPγS and Mg^{2+}, G_s^*, at 10-100pM reproduced the effects of GTPγS. (3) The effects were mimicked by the preactivated α-subunit of G_s, α_s^*. βγ dimers had no effect. (4) G_s^* activation of single Ca^{2+} channel currents was specific. Unactivated G_s, unactivated human erythrocyte G_k and preactivated G_k^* had no effects. (5) G_s treated with activated cholera toxin in the presence of GTP, NAD^+ and ADP-ribosylation factor reproduced the G_s^* effects. Thus in addition to indirect activation through cytoplasmic second messengers the stimulatory G protein, G_s^*, directly activates Ca^{2+} channels in skeletal muscle.

Supported by AHA 851159 and HL 31164.

M-AM-D8 INTERACTIONS BETWEEN A PROTONATION SITE AND AN ION-BINDING SITE IN THE PERMEATION PATH OF THE DIHYDROPYRIDINE SENSITIVE CA-CHANNEL. Daniela Pietrobon, Blaise Prod'hom & Peter Hess, Dept. of Physiology & Biophysics, Harvard Medical School, Boston, MA 02115.

Under appropriate conditions (+ (S) 202-791, absence of divalent ions) discrete transitions between the fully open and a lower (partially blocked) current level can be resolved in single cardiac L-type Ca channels. The transitions result from binding and unbinding of individual proton or deuterium ions to a single site on the channel, since the number of blocking transitions increases linearly with the activity of H^+ or D^+ ions. The rate constants of proton binding (k_{on}) and unbinding (k_{off}) have been estimated with different permeant ions. k_{off} strongly depends on the species of the permeant ion: the smaller the permeant ion, the higher the value of k_{off}. The mean dwell time of a proton at the site increases from 50 μs with Na to 200 μs with K and 800 μs with Cs. The extremely high k_{on} ($\sim 5 \times 10^{11}$ $(Msec)^{-1}$) is similar with different ions. The pK of the site changes from 8.6 with Cs to 8 with K and 7.4 with Na. As the concentration of the permeant ion decreases, the pK increases as a result of both an increase in k_{on} and a decrease in k_{off}. The dependence of k_{off} on species and concentration of permeant ion strongly suggests an interaction (perhaps through a conformational change) between the ion binding site and the protonation site.

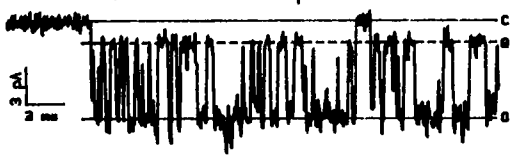

M-AM-D9 SIMULTANEOUS MEASUREMENT OF INTRACELLULAR CALCIUM AND MEMBRANE CURRENTS OF SINGLE GH_3 CELLS HELD UNDER VOLTAGE-CLAMP. C.D. Benham, Department of Pharmacology, Smith Kline & French Research Limited, The Frythe, Welwyn, Hertfordshire AL6 9AR, U.K.

GH_3 cells are a prolactin secreting, pituitary cell line, where secretion is thought to be dependent on intracellular calcium (Ca_i). GH_3 cells were held under voltage-clamp using standard patch-clamp techniques (Pipette solution (mM): 130 Cs Cl, 10 Hepes, 4 Mg Cl_2, 2 ATP, 100 μM EGTA, 50 μM INDO-1 K-salt, TEA-OH to pH 7.2). Ca_i was calculated from the ratio of the fluorescence of INDO loaded cells at 480 and 405 nm measured simultaneously with two Photomultiplier tubes.

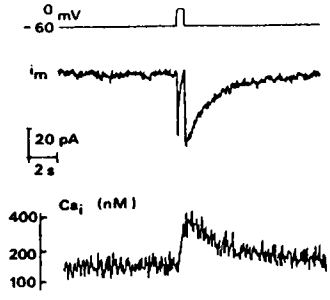

Cells held at -60 mV in a bathing solution containing 1 mM Ca at 25°C had a Ca_i of about 100 nM. Depolarising voltage steps activated voltage gated inward currents and a transient rise in Ca_i (Fig). The rise in Ca_i relative to test potential was bell shaped with a peak close to 0mV suggesting a dependence on Ca entry. Rise times of Ca_i transients were 200-700 ms which may partly reflect diffusion of Ca into the bulk cytoplasm. The decay was monoexpotential with time constants between 3 and 6 seconds. In unclamped cells loaded with 0.5 μM INDO-AM ester, spontaneous Ca_i transients with similar temporal properties were seen presumably due to spontaneous action potential firing.

M-AM-D10 G PROTEIN MODULATION OF CALCIUM CHANNELS INDUCES PROLONGED BACKWARD SWIMMING IN PARAMECIUM. Anita D. McIlveen and Barbara E. Ehrlich. Departments of Medicine and Physiology, University of Connecticut, Farmington, CT. (Intr. by Arnold M. Katz).

We tested compounds that may modulate Ca channels in Paramecium calkinsi by measuring the duration of backward swimming in Paramecium. This behavior correlates with the magnitude of the voltage-dependent Ca current. To incorporate putative regulatory compounds intracellularly, cells were reversibly permeabilized with EDTA. Test compound(s) then were incorporated with 6-carboxyfluorescein, a permeabilization indicator, and cells were resealed with $MgCl_2$. The effect of the test compound on the duration of backward swimming of fluorescent cells was measured after the cells were induced to swim backward by depolarizing them with high potassium. We found that intracellular concentrations of $\geq$1 uM GTPγS, a nonhydrolyzable analog of GTP which activates G proteins, caused the cells to swim backward irreversibly (>900 seconds). Mean recovery time for control cells was 180 seconds. Other compounds such as GDPβS, ATPγS, AMPPNP, and GMPPNP (each at 100 uM) had no effect suggesting that the action of GTPγS is specific. Addition of the Ca channel blocker W-7 before depolarization of the cells prevented backward swimming regardless of the presence of GTPγS, indicating that Ca is needed to trigger the behavior. When W-7 was added 300 seconds after depolarization, the GTPγS-treated cells started to swim forward which suggests that Ca influx through the Ca channel is maintained throughout the prolonged backward swim seen in GTPγS-treated cells. Preliminary data suggest that intermediate steps in modulation of this channel are a decrease in cAMP levels and activation of a kinase. BEE is a PEW Scholar in the Biomedical Sciences.

M-AM-D11 EXOCYTOSIS-SPECIFIC CALCIUM CHANNELS OF DIFFERENT SENSITIVITIES TO VERAPAMIL AND CADMIUM Alice L. Vuoso, Birgit H. Satir, Department of Anatomy and Structural Biology, Albert Einstein College of Medicine, Bronx, New York.

The involvement of Ca^{2+} channels in stimulus-exocytosis-coupling in Paramecium tetraurelia was shown earlier by a dose- and time-dependent inhibition of exocytosis of trichocyst matrices (tmxs) using the Ca^{2+} antagonist verapamil. In addition an intermediate response of secretion in verapamil was demonstrated in which the anterior portion of the cell released tmxs while the posterior was inhibited (A^+P^-) (Vuoso and Satir, Biophys.J. 49:200a, 1986). Exposure to the Ca^{2+} channel blocker Cd^{2+} also inhibited secretagogue induced exocytosis, but unlike verapamil, the intermediate secretory response was P^+A^-. Cells stimulated without blockers in the presence of less than the minimum requirement of Ca^{2+} (< 0.4mM), showed neither A^+P^- nor P^+A^- intermediate stages of release, but rather an overall reduction in numbers of tmxs which were released randomly from the cell surface. These results suggest different Ca^{2+} channel sensitivities to the blockers. Extracellular Ca^{2+} is required since cells in a Ca^{2+}-free buffer could be stimulated to secrete if the secretagogue itself contained millimolar Ca^{2+}. Mg^{2+}, Ba^{2+}, Na^+ and K^+ were unable to substitute for Ca^{2+} in the exocytosis response. The specificity of these channels for exocytosis was confirmed using the Paramecium mutant with defective ciliary Ca^{2+} channels (Pawn A, $d4_{500}$) which responded to secretagogue identically to wild type cells. Thus, these exocytosis Ca^{2+} channels are not the ciliary Ca^{2+} channels. In thin section electron microscopy wild type cells inhibited by verapamil and stimulated with secretagogue showed trichocysts docked at the plasma membrane similarly to unstimulated control cells. Supported by grants from NIH.

M-AM-D12 KINETICS OF Ca^{2+}-INDUCED Ca^{2+} CHANNEL INACTIVATION AND BLOCK, USING "CAGED" Ca^{2+} IN DORSAL ROOT GANGLION NEURONS. M. Morad, J.H. Kaplan, N.E. Davies and H.D. Lux. Dept. of Physiology, Univ. of Pennsylvania, Philadelphia, PA and Max Planck Inst., 8033 Planegg FRG.

1-2 days old dorsal root ganglion neurons were voltage-clamped using the whole cell clamp technique. DM-nitrophen, a photolabile tetraacetic acid Ca^{2+} chelator, was either introduced into the neurons by including it in the patch pipet or was added to the extracellular solutions. DM-nitrophen changed its Ca^{2+} binding affinity from $3x10^{-8}$ to $2x10^{-3}$M on photolysis releasing the caged Ca^{2+} (Kaplan and Ellis-Davies, Biophys. J. this vol.). Intracellular solutions contained high concentration of Cs^+ and were buffered at pH 7.0 with 20 mM Hepes. Current through the Ca^{2+} channel was measured by 70 ms depolarizing pulses to zero mV from a holding potential of -90 mV. Resting $[Ca^{2+}]_i$ were buffered to $>10^{-7}$M using DM-nitrophen plus Ca^{2+}, measured with Ca^{2+} microelectrodes. Photolysis of "caged" Ca^{2+} with a light pulse (150 us; 3mJ/mm^2), photo released 50-100 uM Ca^{2+}. We examined the kinetics of Ca^{2+}-induced inactivation of the Ca^{2+} channel using Ca^{2+}, Ba^{2+}, Na^+ as current carriers. When Ca^{2+} or Ba^{2+} carried the current, photorelease of Ca^{2+} enhanced the inactivation kinetics with a half-time of 5ms. If the current through the Ca^{2+} channel was carried by Na^+, the Ca^{2+} induced inactivation was markedly faster ($t_{1/2}$ 0.56 ± 0.12 ms). The degree of the reduction in i_{Ca} ranged from 35-100% in different cells. In the Na^+ transporting state, extracellular photorelease of Ca^{2+} blocked the Ca^{2+} channel with similar kinetics, $t_{1/2}$ of 0.35ms. Our studies show that Ca^{2+} induced inactivation of Ca^{2+} channel is dependent on the valency of the permeating ion, suggesting that either the permeating ions affect access to the blocking site or that channel structure is altered by the permeating ion.

M-AM-D13 INFLUENCE OF HOLDING POTENTIAL ON PROPERTIES OF Ca^{2+} CURRENT IN FROG VENTRICULAR CELLS. V.J.A. Schouten and M. Morad. Dept. of Physiology, University of Pennsylvania, Philadelphia, PA, 19104.

Isolated frog ventricular myocytes were voltage clamped using the whole-cell patch-clamp technique. Na^+ current was blocked with 1 uM TTX and the remaining inward current was identified as I_{Ca}, since it was blocked by Ni^{2+} and altered by $[Ca^{2+}]_o$. The influence of holding potential on I_{Ca} was tested by applying 100 ms voltage-clamp pulses to +10 mV at a rate of 0.1 Hz from the holding potential. With a holding potential of -90 mV the amplitude of I_{Ca} was stable for several hours. At -40mV holding potential, however, the elicited I_{Ca} gradually decreased in two exponential phases with time constants of about 40 s and 10 min. The slow phase was irreversible and was thought to be related to the phenomenon generally termed "rundown." The rapid phase was reversible upon returning the holding potential to -90 mV within 1 min. This novel phenomenon seems to be a very slow type of inactivation that occurs at membrane potentials at which I_{Ca} is not activated (-70 to -30 mV), i.e., at more negative potentials than the classical type of inactivation. The role of intracellular Ca^{2+} in the very slow inactivation was tested with the following interventions: (a) substitution of Ba^{2+} for extracellular Ca^{2+}; (b) reduction of I_{Ca} by 10 mM Mg^{2+}; (c) enhancement of I_{Ca} by cAMP, or (d) high $[Ca^{2+}]_o$. Though these interventions were expected to reduce or increase the level of intracellular Ca^{2+}, we found no significant effect on the kinetics of the very slow inactivation, suggesting that a $[Ca^{2+}]_i$ independent process was responsible for the very slow inactivation of I_{Ca}.

M-AM-D14 AMILORIDE SELECTIVELY BLOCKS THE LOW THRESHOLD (T) CALCIUM CHANNEL. Cha-Min Tang and M. Morad, University of Pennsylvania, Dept. of Physiology, Philadelphia, PA 19104.

More than one type of voltage-gated calcium channel has been identified in muscle and neurons. Although many blockers of the high threshold (L) calcium channel are known, no specific blocker of the low threshold (T) channel has been identified. Using the whole-cell patch-clamp technique in cells dialyzed with Cs^+ and TEA, and bathed in solutions of 5mM Ca^{2+} and TTX (10^{-6}M), we found that amiloride, a K^+ sparing diuretic, blocked selectively the T channel in mouse neuroblastome (N18) and chick DRG neurons. In the neuroblastoma cells the K_d for amiloride block of the T channel current was 30uM. The onset of the drug action was <1s and the effect was reversible. At concentrations >500uM amiloride had a small <20% effect on the L channel. Amiloride when introduced inside the cell had no effect on i_{Ca}. Amiloride also reversibly blocked the Na^+-conducting T channel current in both the neuroblastoma and DRG neurons. The selective blockade of the T channel was also seen in guinea pig ventricular (Dukes, Naebauer & Morad, unpublished observations) and GH_3 cells. Our results suggest that amiloride specifically blocks the T channel in a variety of cell types supporting the idea that the low threshold channel is a distinct molecular entity different than the high threshold channel.

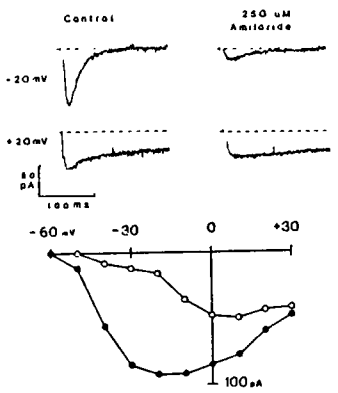

M-AM-E1 STUDY OF ADP-RELEASE STEP IN CHEMICALLY SKINNED SINGLE RABBIT PSOAS FIBERS. M. Kawai and T.W. Cornacchia. Department of Anatomy, The University of Iowa, Iowa City, IA 52242.

To study the nature of interaction between myosin crossbridges and MgADP molecules in skinned fiber system, incremental concentrations of MgADP was introduced to activating saline in the presence of myokinase inhibitor AP_5A (0.1mM), and in the absence of ATP-regenerating system. The experiment was carried out in 1mM excess Mg^{++}, 1-10mM MgATP, 2-8mM Pi (phosphate), 5mM CaEGTA (pCa 4.5), 200mM ionic strength (K propionate), 10mM MOPS (pH 7.00) and at 20°C. The isometric tension and the three exponential processes deduced from small sinusoidal length oscillations were followed. Tension was minimally affected by MgADP when 8mM Pi was present in the activating saline, whereas it increased with MgADP at a lower concentration of Pi (2mM). The rate constants of both processes (B) and (C) diminished similarly with the increase in MgADP concentrations, whereas the effect on process (A) was very small. The results are consistent with a scheme in which MgATP and MgADP compete for the binding site. From this measurement, the second order rate constant of MgADP binding to myosin crossbridges is deduced to be $7.8\pm1.4 \times 10^4\ M^{-1}sec^{-1}$ (N=8, SEM). When MgADP was added to a rigor fiber in the presence of 1mM glucose and 20 unit/ml hexokinase (to remove contaminating ATP in the ADP solution), no change in tension was observed regardless of the Pi concentration or the presence of oscillation. These results indicate that, once the rigor state is established, either the crossbridges are inaccessible for MgADP binding, or actin-myosin-ADP complex is different from that generated by the addition of MgADP to the cycling crossbridges in mM concentrations of MgATP.

M-AM-E2 EVIDENCE FOR A NOVEL 30 TO 50,000-M_r COFACTOR IN THE ACTIVATION OF MUSCLE
J. Gulati and A. Babu
Division of Cardiology, Albert Einstein College of Medicine, Bronx, NY 10461

When the skinned fibers from the fast-twitch skeletal muscle are subjected to extensive TnC-extraction treatment to release all the TnC, the fibers also lose 50% of the LC2 (Babu et al, BJ.51:320a, 1987). When such OTnC fibers were reloaded with LC's and TnC, we found that there was full tension recovery in low salt (40mM, pCa4) but relatively little or none in high physiological salt (190mM, pCa4). This suggested that an additional factor was lost during the extended TnC-extraction treatment that was essential for the activation of muscle in high salt. Here we present results of new studies to characterise this factor — termed cofactor for activation. The presence of the novel cofactor was confirmed by incubating the (TnC+LC)-loaded fibers with muscle soup, since the tension in high salt was fully recovered with this treatment. With a series of filtrations, using Amicon ultrafiltration membranes, the activity in the soup was found to be confined to 30,000 to 50,000 M_r region. Further, as judged by the ability to restore activity in high salt, the cofactor was present in cardiac muscle, soleus muscle and the brain, but not in the kidney and liver soup. The cofactor was inactivated by heating to 80°C, and also by trypsin treatment at room temperature, indicating that it was a protein molecule. Experiments are underway to establish whether calmodulin can substitute for the cofactor; this is an issue since brain is extremely rich in calmodulin. Amongst several possibilities it is suggested that cofactor is the switch that triggers the weak conformations in the cross-bridge cycle, and/or that this cofactor modulates tropomyosin interaction with thin filament under physiological conditions.

M-AM-E3 INCREASED RATE OF TENSION REDEVELOPMENT AT SUBMAXIMAL [Ca^{2+}] IN FAST-TWITCH SKELETAL MUSCLE FOLLOWING MYOSIN LIGHT CHAIN PHOSPHORYLATION. Joseph M. Metzger+, Richard L. Moss+, Gary G. Giulian+, and Marion L. Greaser*. Department of Physiology+ and the Muscle Biology Laboratory*, University of Wisconsin, Madison, WI 53706.

The Ca^{2+}-sensitivity of the rate constant for tension redevelopment (k_{tr}) was examined in fast-twitch rabbit psoas and rat superficial vastus lateralis (svl) skinned single muscle fibers before and after phosphorylation of myosin LC_2 (LC_2-P). Fibers were maximally Ca^{2+} activated (pCa 4.5) six times in the presence of 0.1 mg/ml calmodulin and 30 µg/ml myosin LC kinase. This protocol was found to produce 80+% LC_2-P as determined by isoelectric focusing. k_{tr} was determined using a modification of the technique of Brenner and Eisenberg, (PNAS 83, 3546, 1986). Control k_{tr} values at pCa 4.5 and 15°C were 26 ± 1 (x ± SE, n=7) and $20\pm1\ sec^{-1}$ for svl and psoas fibers, respectively. k_{tr} and isometric tension were unchanged at pCa 4.5 following LC_2 phosphorylation; however, at submaximal [Ca^{2+}] there were significant increases in isometric tension and k_{tr} in both the psoas and svl fibers. For example, in psoas fibers at pCa 6.0, k_{tr} values (relative to controls at pCa 4.5) were 0.33 ± 0.03 in controls and 0.43 ± 0.05 following phosphorylation. Relative isometric tension values at pCa 6.3 were 0.27 ± 0.06 in controls and 0.41 ± 0.05 following phosphorylation. These results may be interpreted in terms of a LC_2-P dependent increase in the rate of cross-bridge attachments in fast-twitch fibers leading to enhanced cooperative activation of the thin filament and increased isometric tension at submaximal [Ca^{2+}]. Supported by NIH.

M-AM-E4 CROSSBRIDGE CONFORMATIONS IN DEMEMBRANATED MUSCLE FIBRES STUDIED BY COMBINED BIREFRINGENCE AND X-RAY DIFFRACTION MEASUREMENTS. M Peckham* and M Irving#. #Dept. of Biophysics, K.C.L., London WC2B 5RL, UK. *HSW-841, C.V.R.I., U.C.S.F., San Francisco Ca 94143.

The birefringence of a muscle fibre is sensitive to the orientation of the crossbridges (Irving, (1984) J.Physiol. 353, 64P). However, applications of the technique have been limited by the fact that birefringence also depends on interfilament spacing. We have now made parallel measurements of birefringence and the equatorial part of the X-ray diffraction pattern from the same single fibre segment. Direct measurement of interfilament spacing allows isolation of the orientation component of the birefringence signal, which can be interpreted in terms of S-1 orientation, using a simple model for crossbridge structure.

Results from the relax-rigor transition in mechanically skinned frog semitendinosus (μ=0.2M, 10°C) and chemically skinned rabbit psoas (μ=0.1M, 15°C) fibres confirmed previous conclusions (Irving & Peckham (1986) J.Physiol. 377, 95P) based on the use of published X-ray data to interpret birefringence changes: the mean angle between the long axis of the S-1 head and the filament axis is about 30° in relaxed and 50° in rigor muscle. A birefringence decrease of about one third of that associated with the relax-rigor transition was produced either by cooling (15° to 5°C, μ=0.1M) or lowering the ionic strength (0.1 to 0.02M, 5°C) of relaxed rabbit psoas fibres. In each case the equatorial intensity ratio $I_{1,1}/I_{1,0}$ increased. Thus all three transitions from the high temperature, high ionic strength relaxed state - removal of ATP, cooling or lowering of ionic strength - result in decreased alignment of crossbridges with the filament axis together with a transfer of mass towards the vicinity of the thin filament. (Supported by the Royal Society and Wellcome Trust.)

M-AM-E5 CHARACTERIZATION OF ACTOMYOSIN CROSS-BRIDGES IN THE PRESENCE OF MgATPγS USING MECHANICAL AND X-RAY DIFFRACTION APPROACHES. B. Brenner, Th. Kraft, & L.C. Yu*. Institute of Physiology II, University of Tübingen, FRG.; *NIAMS, NIH.

To determine whether cross-bridges in the presence of the ATP analogue ATPγS represent "weak-binding" cross-bridge states or should rather be considered "strong-binding" cross-bridge states, we compared their mechanical and structural characteristics with those of cross-bridges in relaxed fibers and in the presence of $MgPP_i$ as representatives of weak- and strong-binding states respectively. Using single skinned rabbit psoas fibers, it is found from measurements of fiber stiffness and of the first two equatorial reflections that the properties of cross-bridges in the presence of ATPγS closely parallel the properties of cross-bridges in the presence of $MgPP_i$; (1) actin attachment of cross-bridges is stronger than in relaxed fibers, as indicated by the higher apparent fiber stiffness and the higher ratio $I_{1,1}/I_{1,0}$ at all ionic strengths, (2) attachment to actin is not as rapidly reversible as in relaxed fibers, indicated by the left-shift when apparent fiber stiffness is plotted vs. speed of the stretches applied for stiffness measurements, (3), and most importantly, in the presence of ATPγS cross-bridge attachment is Ca^{++}-sensitive and cooperative. Lowering ionic strength or raising temperature in the absence of Ca^{++} leads to a steep increase in apparent fiber stiffness and in $I_{1,1}/I_{1,0}$, up to the values observed in the presence of Ca^{++} (pCa 4.5) under the same conditions. This indicates that attached cross-bridges in the presence of ATPγS, different from attached cross-bridges in relaxed fibers, can turn on the contractile system in the absence of Ca^{++}, the key property which distinguishes weak- from strong-binding cross-bridge states. Control experiments show that the observed turning on of the contractile system is not due to ADP contamination, incomplete saturation with ATPγS, or insufficient Mg^{++}-concentration. (DFG, Br 849/1-2).

M-AM-E6 CALCIUM INDUCED TRANSITIONS BETWEEN CROSS-BRIDGE BINDING STATES, WITHOUT NUCLEOTIDE HYDROLYSIS. A.J. Baker and R. Cooke, Dept. of Biochem/Biophys and the CVRI, Univ of California, San Francisco, CA. 94143.

The non-hydrolysable nucleotide ATPγS, at 1mM, causes complete relaxation of glycerinated rabbit psoas muscle fibers at normal ionic strength, 5°C, and pH 7.0. The tension and stiffness (measured during stretches (0-2 % in 2ms) and oscillations (+/- 2%)) are zero and the EPR spectra of SH1 probes indicate complete angular disorder. We estimate from our measured binding constant that greater than 97% of S1s have a nucleotide bound and that the fraction of rigor is negligible. When the ionic strength is lowered (20mM) cross-bridges become attached to actin. The fiber stiffness rises to 20% of rigor and shows a frequency dependence to oscillations between 0.1-100 Hz. From 100-1000 Hz the stiffness is frequency-independent. Addition of calcium does not result in significant force development but the fiber stiffness rises to 50% of rigor, whilst there is only a small increase (15%) in the fraction of ordered EPR probes. The ordered probes have the same orientation as found in rigor. The stiffness increase also has a frequency dependence in the 0.1-100 Hz range, unlike rigor stiffness which is frequency independent. Raising the ionic strength of the bathing solution by addition of 120mM KAc causes only a small reduction in the stiffness to about 35 % of rigor. In conclusion, addition of calcium allows an increase in the fraction of cross-bridges binding more strongly to actin. This fraction is small compared to the much larger increase in stiffness. Calcium can control a step in the cross-bridge cycle much earlier than has previously been supposed. Supported by USPHS AM30868.

M-AM-E7 **'DOUBLE CAGE' ACTIVATION OF SINGLE SKINNED MUSCLE FIBERS FROM THE FROG BY THE SIMULTANEOUS RELEASE OF ATP AND CALCIUM FROM CAGED-ATP AND NITR-5.**

C.C. Ashley[+], R.J. Barsotti [$], M.A. Ferenczi, T.J. Lea[+] and I.P. Mulligan [+]. *N.I.M.R., London, NW7 1AA. [+] University Laboratory of Physiology, Oxford OX1 3PT. [$] Bockus Institute, Philadelphia, PA 19146.*

We have studied the influence of rigor cross-bridges on the rate of calcium-mediated force development, with a 'double cage' experiment in which both ATP and calcium were released concurrently by a single pulse of laser light. Photolysis of 2mM caged-ATP and 3mM nitr-5 (initial pCa6.6, pH7.0, 13°C I= 0.2M, pMg2.7) in a single permeabilised (Triton X100 0.5% v/v) fibre from the semitendinosus muscle of the frog, *Rana temporaria*, by a pulse of laser light (75mJ in <200ns at 347nm) released 1mM ATP and also raised the pCa to 5.8, causing full isometric force to develop from rigor with a mean $t_{1/2}$ = 19 ± 1ms (s.e.m., n=5). This is faster than the rate following photolysis of nitr-5 alone in the presence of 5mM MgATP ($t_{1/2}$ = 40 ± 2ms, n=11), but it is similar to the rate following photolysis of caged-ATP at pCa 4.5 ($t_{1/2}$ = 22 ± 2ms, n=8). When caged-ATP is photolysed in the absence of calcium (pCa>8.0), thin filament activation decays as cross-bridges detach. The rate of rise of force following 'double cage' photolysis is similar to that observed when caged-ATP (pCa≤4.5) alone is photolysed. This similarity in rates implies that in the 'double cage' experiment, calcium-mediated activation of the thin filament is rapid compared with the rate of decay of thin filament activation following the detachment of rigor cross-bridges.(Supported by N.I.H. R01-AR37701-021, M.D.A. and S.E.R.C.)

M-AM-E8 **ACTIVATION OF SKELETAL MUSCLE FIBERS BY PHOTOLYSIS OF DM-NITROPHEN, A NEW CAGED Ca^{2+}**

Y.E. Goldman and J.H. Kaplan, Department of Physiology, School of Medicine, University of Pennsylvania, Philadelphia, PA 19104

DM-nitrophen binds Ca^{2+} and Mg^{2+} with K_d's 27 nM and 3 μM respectively at pH 6.9 (Kaplan & Ellis-Davies, this volume). Photolysis by u.v. radiation splits DM-nitrophen into two iminodiacetic acid moieties with release of bound Ca^{2+} and Mg^{2+} on the sub-millisecond time scale (K_d's > 1 mM). Glycerol-extracted single fibers from rabbit psoas muscle were fully relaxed in 100 mM TES, 2 mM DM-nitrophen, 1.2 mM total Mg, 1.0 mM total Ca, 1.4 mM ATP, 10 mM glutathione, 29.4 mM HDTA and 20 mM creatine phosphate, pH 7.1, 200 mM ionic strength, 20°C. A single pulse (~130mJ) from a frequency-doubled ruby laser into a 23 μl fiber trough photolyzed ~25% of the DM-nitrophen, causing full activation. Tension increased within 1-2 ms of the laser pulse (arrow in Fig.) and reached a plateau with $t_{1/2}$ as short as 17 ms. Stiffness (2 kHz) rose ~5 ms earlier than tension at the half-plateau value. Reducing the laser pulse energy decreased the steady levels of tension and stiffness and their onset rates. The properties of DM-nitrophen as a caged Ca^{2+} will enhance temporal resolution in studies of Ca^{2+} activation.

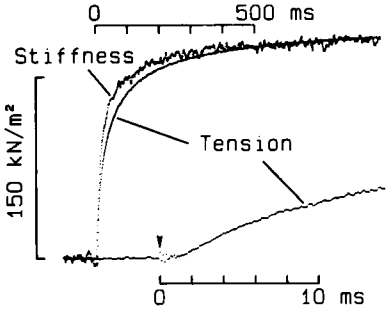

Support: MDA and NIH grants HL15835 to the PMI and HL30315.

M-AM-E9 **SARCOMERE MATRIX OF SKELETAL MUSCLE: THE ROLE OF THICK FILAMENTS IN THE SEGMENTAL EXTENSIBILITY OF ELASTIC TITIN FILAMENTS.**

Kuan Wang & John Wright. Clayton Foundation Biochemical Institute & Department of Chemistry, The University of Texas at Austin, Austin, TX 78712

Using monoclonal antibodies to titin as structural probes of the sarcomere matrix of skeletal muscle, we have reported previously that titin filaments, each a single titin molecule extending from M-line to Z-line in a bipolar direction, is stretchable only in the I-band but not in the A-band in intact sarcomeres (JCB 99 435a; BJ 47 349a). Whether this segmental extensibility is intrinsic to titin molecules or imposed by physical interactions with noncompliant thick filaments or other A-band components remains an open question. In the present study, we monitored the behaviors of A-band epitopes of titin in both salt-extracted rabbit psoas muscles of various thick filament lengths, and in highly stretched muscles where distal portions of thick filaments have disassembled or extended, presumably by excessive stress exerted by titin filaments. In both cases, epitopes within A-segments of various lengths remain stationary but exhibit elastic-stretch dependence when outside the A-segments. Removal of the M-line by extraction with 0.6 M KCl dislodged titin and caused most A-epitopes to translocate and accumulate at the edges of I-bands. These data support the notion that the titin filament is intrinsically elastic along its length and that its segmental extensibility in the sarcomere results from strong multiple interactions along parallel thick filaments. (Supported in part by NIH DK20270 and an American Heart Association Established Investigatorship.)

M-AM-E10 THICK FILAMENT MOVEMENT AND ISOMETRIC TENSION IN ACTIVATED SKELETAL MUSCLE
Robert Horowits and Richard J. Podolsky, NIAMS, NIH, Bethesda, MD 20892

Last year we reported that thick filaments can move from the center of the sarcomere to the Z-disc in skinned rabbit psoas fibers activated for several minutes. This movement is maximal in sarcomeres less than 2.5 μm long, where resting stiffness is small, but does not occur in sarcomeres longer than 2.8 μm, where resting stiffness is high. This sarcomere length dependence was attributed to the effect of titin filaments, which are elastic elements linking the ends of the thick filaments to the Z-discs and giving rise to the resting tension. However, the slow time course of movement and the observed stability of tension during movement were not completely understood. From the active and resting tension-length relations and the force-velocity relation, we have now modeled the time course of thick filament movement in the presence and absence of titin filaments. The movement exhibits a lag phase, during which the velocity and extent of movement are extremely small. This lag phase is dependent on the initial position of the thick filament and on the properties of the cross-bridges that are stretched during thick filament movement. The experimental data are well fit assuming an initial thick filament displacement away from the center of the sarcomere of about 0.05%. This leads to a lag of approximately 80 seconds before any significant thick filament movement occurs. In the model incorporating titin filaments, this lag is followed by a phase of slow, steady motion during which isometric tension is stable, as experimentally observed; the model excluding titin filaments predicts a phase of acceleration after the lag, accompanied by a 50% decrease in tension. Therefore, the observed time course of movement and tension are consistent only with the model incorporating titin filaments. In addition, the model suggests that the main role of the titin filaments in vivo is to recenter the thick filaments upon relaxation.

M-AM-E11 A-BAND SHORTENING IN FROG SKELETAL MUSCLE Gerald H. Pollack, Ammasai Periasamy, David H. Burns, Karoly Trombitás. Center for Bioengineering, WD-12, University of Washington, Seattle, WA 98195.

While it is broadly accepted that thick filaments do not change length during contraction, not all results agree. No fewer than thirty-five papers published since the mid-fifties, mostly unknown, report substantial A-band or thick filament shortening. A summary of these results is given in Pollack (*Physiol. Rev.* 68:1049-1113, 1983). Many of these papers leave questions unresolved: questions of artifact; questions of whether filament shortening was due merely to passive compression by Z-lines; and questions of whether conditions were really "physiological."

We therefore studied single isolated fibers of frog skeletal muscle, shortening from extended sarcomere lengths (*ca.* 3.2 μm) to intermediate lengths (*ca.* 2.2 μm). To track A- and I-bands during shortening, we used high-resolution polarization microscopy (NA = 1.25), coupled with a digital image processing system. During passive shortening, sarcomere length changes were accounted for almost entirely by changes of I-band width, as predicted by the sliding filament theory. By contrast, during active shortening under essentially identical conditions, sarcomere length changes were accounted for about equally by decreases of width of I-bands and A-bands. Thus, A-bands shortened by 15 - 20% during contraction.

Additional specimens were glutaraldehyde-fixed for electron microscopy. We were cautious to circumvent potential artifacts arising from sectioning direction, shrinkage, and foreshortening. Those specimens fixed prior to contraction had thick filament lengths of 1.61 μm, exceptionally uniform over the field. Those fixed just after activated shortening had variably shortened thick filaments, typically 1.3 - 1.4 μm but as low as 1.25 μm.

Thus, EM and light-microscopy results agree: both show modest but definite thick filament/A-band shortening during contraction under apparently physiological conditions.

M-AM-E12 **EFFECT OF SHORTENING ON FREE INTRACELLULAR CALCIUM DURING THE RELAXATION OF FROG SKELETAL MUSCLE.** M.B. Cannell, Department of Pharmacology (R-189), University of Miami School of Medicine, PO Box 016189, Miami, FL 33101.

Single fibers from frog tibialis anterior were dissected and the photoprotein aequorin injected into them. Aequorin light emission (a function of the free intracellular calcium concentration) was recorded during tetanus relaxation. During nominally isometric relaxation, there was a decrease in the rate of decline of aequorin light emission during the exponential phase of force relaxation (Cannell, J. Physiol. **376** 203, 1986). Laser diffraction recording from the aequorin-injected region showed that internal sarcomere shortening occurred when the rate of decline of aequorin light decreased. Allowing a muscle to shorten (by imposing a length change on the fiber) during relaxation initially caused an increase in aequorin light emission. Following the increase in aequorin light, the overall timecourse of the decline of aequorin light was abbreviated when compared to the control response. The length dependence of this effect suggested that if there were no overlap between thick and thin filaments then shortening would have no effect on free calcium during relaxation. Computer simulation suggested that these results can be explained by the affinity of troponin for calcium decreasing about 8 fold during rapid active shortening. Thus, naturally occurring length changes during relaxation may help increase the rate of relaxation by causing calcium to unbind from troponin more rapidly. This effect may be mediated via cross bridge attachment affecting the affinity of troponin for calcium.

M-AM-F1 RHEOLOGICAL NORMALCY OF G-ACTIN. Ken S. Zaner[1], Jay Newman[2], Kenneth L. Schick[2], Ruth Furukawa[3], and Bennie R. Ware[3], [1] Hematology-Oncology Unit, Massachusetts General Hospital, Boston, MA 02114, [2] Physics Dept., Union College, Schenectady, N.Y. 12309, [3]Dept. of Chemistry, Syracuse Univ., Syracuse, N.Y. 13244-1200.

Recent reports that dilute solutions of G-actin form viscoelastic gels have been investigated using several experimental variations of three distinct physical techniques in three independent laboratories. The dynamic storage and loss moduli of G-actin solutions were measured using two rheometers of different design over periods of up to 15 hours. Measurements of the diffusion of G-actin and of the diffusion of probe particles added to G-actin solutions were performed over periods of many hours, to days in some cases, using both dynamic light scattering and fluorescence photobleaching recovery techniques. Actin solutions were prepared independently in the three laboratories under conditions for which anomalous gelation had been reported. We find no evidence for gelation of G-actin solutions, our data being consistent only with the conclusion that G-actin solutions behave as normal Newtonian liquids.

M-AM-F2 PROFILIN SEQUESTERS G-ACTIN MORE WEAKLY FROM THE BARBED THAN FROM THE POINTED FILAMENT END. Weber A, Southwick F, Young C, Rosenbaum H and Mooseker M. Dept. of Biochemistry and Biophysics, & Dept. of Medicine, University of Pennsylvania, & Dept. Biology, Yale University.

Tilney et al (1983, J Cell Biol 97, 112) and Kaiser et al (1986, J Cell Biol 102, 221) showed that Acanthameba profilin interfered little with actin filament elongation at the barbed filament end. However, Kaiser et al found that the apparent Kd of profilin for G-actin decreased from about 50 to 10uM when the effect of profilin on the steady state G-actin concentration (barbed filament ends free) was measured. By contrast, Lal and Korn (1985, J Biol Chem 260, 10132) observed no difference in the actin sequestering ability of this profilin with regard to the inhibition of filament elongation (at both ends simultaneously) and the increase in steady state G-actin.

A comparison of the effect platelet profilin on monomer binding to the barbed and to the pointed filament end showed profilin to be much more effective against the pointed end. Profilin sequestered monomers with an apparent Kd of about 2-3uM from villin-capped actin filaments (= pointed ends) both with regard to a) inhibition of elongation rate and b) increase in steady state [G-actin]. By contrast, a much higher apparent Kd of 17-21uM for profilin-actin binding was obtained from the inhibition of the elongation rate of limulus acrosomes in the presence of 0.5uM G-actin (subcritical for the pointed end) and the increase in steady state [G-actin] when the barbed filaments were uncapped. Steady state [G-actin] was obtained both by nucleated polymerization (without nuclei, endpoints in the presence of profilin could not be obtained even after 48h incubation) and by depolymerization of F-actin.

M-AM-F3 ORIENTATION OF ACTIN MONOMER IN THE F-ACTIN FILAMENT. NEW RADIAL COORDINATES AND THE EFFECT OF S1 BINDING ON MONOMER ORIENTATION. Andrzej A. Kasprzak, Reiji Takashi, and Manuel F. Morales, CVRI, University of California, San Francisco.

Fluorescence resonance energy transfer (FRET) measurements have been used to orient actin monomers in the F-actin filament. The distance between two equivalent chemical points located on different monomers was measured and used subsequently to compute the radial coordinate of this point.If radial cooordinates of 4 points are determined and 6 intramolecular distances are known from (from x-ray crystallography or FRET), one can, within symmetry limits, position the monomer about the filament axis. The radial distance of Gln-41 which had been enzymatically modified with dansyl, rhodamine, and fluorescein derivatives of cadaverine was found to be ~40-42 Å. Monobromobimane and 1,5-IAEDNS as donors and DABM as acceptor were used to label Cys-374. The results yielded a radial coordinate of this residue in the range 20-25 Å. The effect of S1 binding on the radial coordinates of: 1) Gln-41, 2) Cys-374 3) the nucleotide binding site was examined. S1 had a small effect on Gln-41 increasing it to 44-47 Å. The change of radial coordinates of the two other residues caused by S1 binding was negligible. (Supported by NSF PCM 8316007 and NIH HL-16683.)

M-AM-F4 FLUORESCENT LABELLING OF ACTIN WITH RHODAMINE-X-MALEIMIDE. Cris dos Remedios, Sean O'Donohue, Julian Barden and Masao Miki, Muscle Research Unit, Department of Anatomy, The University of Sydney, Sydney, 2006, AUSTRALIA.

Skeletal muscle contains five cysteine residues, one of which (Cys-374) can be readily labelled by cysteine-directed fluorescent probes. The labelling of other cysteines (e.g. Cys-10; Barden et al. 1986, Biochem. Int. 12: 95-101) requires protein-modifiers e.g. 1-2M urea. At pH 7.0, 2 moles of rhodamine react with each mole of actin at 23°C over 24 hrs in the absence of urea. By comparison, using other labels (e.g. IAF, NBD, AEDANS), only one mole of label reacts with each mole of actin under the same conditions. Because of the extremely hydrophobic nature of rhodamine, this observation suggests that the second label site resides in a predominantly hydrophobic region of actin. When Cys-374 is blocked by NEM (5 fold molar excess for 30 minutes at 25°C) the labelling stoichiometry for the rhodamine does not exceed 1:1. Such actin only poorly activates the ATPase activity of myosin. In contrast, binding studies of rhodamine-F-actin to either S-1 or HMM show no significant difference from control actin. These data suggest that the new (i.e. second) rhodamine labelling site is near to but not actually at the myosin binding site. The precise location of the second rhodamine site is unknown but studies are in progress to establish this definitively.

This research was supported by the NH&MRC of Australia.

M-AM-F5 TRANSIENT NETWORK ANALYSIS OF CYTOSKELETAL ELASTICITY.
Ralph Nossal, Physical Sciences Laboratory, DCRT, NIH, Bethesda, Maryland 20892.

The dynamic nature of molecular bonding in cytoplasmic networks can result in time-dependent relaxation of mechanical stress imposed upon such structures. Transient network models of polymerizing actin filaments, which explicitly incorporate crosslinking by Actin Binding Protein and other factors, are analyzed mathematically. Expressions are obtained for viscoelastic coefficients in terms of kinetic constants and the concentrations of network constituents. The appropriateness of using dynamic light scattering for in vitro determinations of shear storage and loss moduli is examined, and conditions necessary for the resolution of spectral data are discussed. A scheme is proposed in which elasticity measurements are used to distinguish between possible kinetic mechanisms of network crosslinking effected by alpha-actinin.

M-AM-F6 THE CRYSTAL STRUCTURE OF ACANTHAMOEBA PROFILIN-I AT 2.4 A° RESOLUTION. K.A. Magnus, E.E. Lattman, D.A. Kaiser and T.D. Pollard, Departments of Biophysics and Cell Biology and Anatomy, Johns Hopkins Medical School, Baltimore, MD 21205 USA.

We have determined the crystal structure of Profilin-I from Acanthamoeba at 2.4 A° resolution using multiple isomorphous replacement. The entire course of the polypeptide chain has been traced, although 1 or 2 possible ambiguities remain. The molecule is organized into 2 domains that are connected by a single α-helix running down the page on the left. The upper domain is all α-helix; the lower α- and β-structure. The side chain of lysine 115, which is linked to actin by zero-length cross-linking reagents (T. Pollard, D. Kaiser, C. Ampe & J. Vandekerckhove), is shown top left (↓). The function of the deep cleft between the 2 domains is not known. This work was supported by NIH grants GM-35171 and GM-26338.

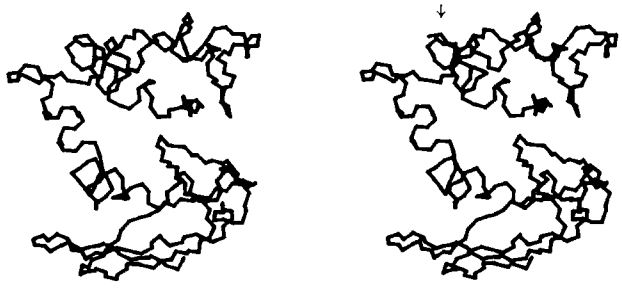

M-AM-F7 Kinesin-Driven Movement on the Nanometer Scale. J. Gelles, B.J. Schnapp and M.P. Sheetz, Washington Univ. Med. School, St. Louis, and Lab of Neurobiology, NINCDS, NIH at MBL, Woods Hole (Intr. by J.E. Brown).

Purified kinesin moves plastic beads along microtubules in vitro in an assay that provides a unique opportunity to study motions induced by a small number of force-generating enzyme molecules [Vale, et al., Cell 42, 39-50 (1985)]. Analysis of the molecular mechanical processes that produce movement in this system requires measurement of bead motions with nanometer-scale precision. We have devised a method to determine the position of a kinesin-driven 150-190 nm diameter bead with a precision of 1-2 nm at 30 Hz. The method is based on digital processing of images from differential interference contrast microscopy and can be implemented using commercially available video and computer equipment. For kinesin-coated beads moving at low (2.5 μ M) ATP concentrations, measured bead positions tend to occur at discrete spacings along the microtubule. Under these conditions, the kinesin-driven beads sometimes execute repeated transient stops spaced 2-4 nm apart on the microtubule axis. In their motions perpendicular to the microtubule axis, individual beads maintain a single circumferential position with respect to the microtubule surface as they move axially over hundreds of nanometers. These results help to explain how microtubules support multiple independent tracks for organelle movement. Taken together, the nanometer-precision measurements of the bead motions reveal basic mechanical features of kinesin-driven motility which place significant constraints on proposed molecular mechanisms of movement.

M-AM-F8 SPLITTING THE CILIARY AXONEME: PATTERNS THAT SUPPORT THE 'SWITCH POINT' MODEL OF CILIARY ACTIVITY. T. Matsuoka and P. Satir, Dept. of Anatomy and Structural Biology Albert Einstein Coll. of Med., Bronx, NY 10461.

We have been investigating a 'switch point' model of ciliary activity based on the finding by Sale and Satir (1977) that dynein arm activity is always polarized. Since active doublet sliding is therefore unidirectional, it must also be asynchronous if the ciliary axoneme is to move. Mussel gill lateral (L) cilia can be stopped in two distinct beat positions -'hands up' and 'hands down'. The model proposes that doublets on only one half of the axoneme are active to reach one of these positions and that doublets on the other half are active to reach the other position. We have attempted to obtain direct evidence for this proposition by studying splitting patterns of hands up and hands down L cilia induced in demembranated axonemes by addition of 4mM ATP. Prior to addition of ATP, axonemes are intact, but addition of ATP disrupts about 40% of the axonemes. In both hands down and hands up axonemes, breaks occurred between specific doublets; the pattern of disruption seen was significantly different in the hands down vs. hands up axonemes. In particular, during disruption in hands down axonemes, the central pair is associated with doublets 3 and 4 in the group 9,1,2,3,4 or 3,4,5,6,7,8. In hands up axonemes, the central pair is associated with doublets 8 and 9 in the group 5,6,7,8,9 or 8,9,1,2,3,4. A simple analysis suggests breaks occur between active and inactive doublets or alternatively between active and attached, immobile doublets. The activity patterns found by this analysis correspond closely to those predicted by the switch-point model. In addition, the data suggest that spoke-central sheath interactions also switch during ciliary beat. Supported by USPHS

M-AM-F9 A MINIMAL MODEL FOR THE ASSEMBLY AND DYNAMIC INSTABILITY OF MICROTUBULES. Peter Bayley, Maria Schilstra and Stephen Martin, Division of Physical Biochemistry, National Institute for Medical Research, Mill Hill, London NW7 1AA, U.K.

The observations (by Horio & Hotani (1986) Nature 321, 605-607) that the steady-state microtubule population comprises constant proportions of growing (G) and shrinking (S) microtubules suggests a minimal model for numerical stimulation of the self assembly and steady-state dynamics of tubulin dimer. We adopt the following propositions : a) there is effectively tight coupling between tubulin subunit addition and GTP-hydrolysis, making any GTP-tubulin cap very small; b) elongation by addition of GTP-tubulin causes hydrolysis of the previously terminal GTP-tubulin subunit; c) the G-state has terminal GTP-tubulin and the S-state has terminal GDP-tubulin and transformations from G to S state (and from S to G) involve respectively the loss (or addition) of terminal GTP-tubulin. These postulates allow a detailed quantitative formulation of several experimental phenomena, including microtubule elongation kinetics, oscillatory growth behaviour, the transient effects of shearing tubulin microtubules, the kinetics and length-dependence of tubulin exchange with steady-state microtubules and length redistributions at steady-state. Specifically, the fast switching of G to S required for fast microtubule dissociation after rapid dilution and the slow switching of G to S required for overshoot and oscillatory behaviour during assembly is accommodated by making the switching process strongly dependent on the concentration of free GTP-tubulin.

M-AM-G1 ACTIVATION OF NEURONAL OXIDATIVE METABOLISM BY CALCIUM IONS

Marcos Tsacopoulos and Alan Fein, Experimental Ophthalmology Laboratory, Geneva, Switzerland and Department of Physiology, University of Connecticut Health Center, Farmington, CT.

Illumination of the Lumulus ventral photoreceptor leads to a transient increase in the cells' intracellular concentration of sodium (Na_i^+) and mitochondrial O_2 consumption (ΔQO_2). After a light flash, ΔQO_2 returns to the preillumination level about five times faster than Na_i^+. Pressure injection of sodium into the cell in order to elevate Na_i to the same levels as attained by illumination does not lead to an increase of the consumption of O_2. We conclude that activation of the sodium pump by a rise in Na_i is not a factor involved in the light induced ΔQO_2. Three observations indicate that the ΔQO_2 results, in part, from a rise in intracellular calcium (Ca_i). There is a light induced rise in $^{45}Ca_i$ that has a similar time course to the ΔQO_2. The calcium buffer, EGTA, tends to block the light induced ΔQO_2. Pressure injection of calcium into the cell induces a ΔQO_2. These findings demonstrate that a rise in Ca_i participates in activation of oxidative energy metabolism in a living neuron.

M-AM-G2 REGULATION OF THE MITOCHONDRIAL INNER MEMBRANE ANION CHANNEL BY Mg^{2+} AND PROTONS.

Andrew D. Beavis, Dept. of Pharmacology, Medical College of Ohio, Toledo, OH 43614.

It has long been known that alkaline pH makes mitochondria permeable to a wide variety of anions. It has also been shown that anion uniport can be activated by depletion of mitochondrial divalent cations using EDTA and the ionophore A23187. Furthermore, this pathway is also regulated by protons with a pI_{50} close to 7.8 (Beavis, A.D. and Garlid, K.D., J. Biol. Chem. 262, (In the press)). We have now begun to investigate the relationship between these two inhibitors.

Anion uniport in mitochondria depleted of endogenous divalent cations is inhibited by Mg^{++}. At low concentrations of A23187 (< 0.2 nmol/mg) mitochondrial swelling in KCl plus valinomycin is inhibited with an I_{50} close to 0.6 mM; however, when A23187 is present at 1 nmol/mg or higher, the I_{50} decreases to about 50 μM. Thus, there appears to be a high affinity inhibitory site on the inner surface of the membrane.

Mg^{++} inhibits at all pH values tested; however, the I_{50} increases from the value of 50 μM at pH 7.4 to about 300 μM at pH 8.4. This finding could explain the observation that extreme alkaline pH is sufficient to activate anion uniport. These results are consistent with a model in which the putative anion uniporter must be protonated at a site with a pK < 7 before Mg^{++} can bind to a site with a K_I close to 10 μM. Since the pK of this proton binding site appears to be lower than that of the inhibitory site two distinct protonation sites may exist; one involved in regulation of transport and the other involved in regulation of Mg^{++} binding. This model provides a mechanism to increase the sensitivity of anion uniport to pH. This research was supported by NIH grant HL 36573.

M-AM-G3 ION TRANSPORT IN MITOCHONDRIA: THE BASIS FOR NON-LINEAR FLUX-FORCE RELATIONSHIPS.

Keith D. Garlid, Paal Falnes and Signe Kjelstrup Ratkje*, Department of Pharmacology, Medical College of Ohio, Toledo, OH 43699. (*On leave from Division of Physical Chemistry, Norwegian Institute of Technology, N-7034 Trondheim-NTH, Norway.)

We have measured valinomycin-induced potassium efflux from non-respiring rat liver mitochondria under conditions where K^+ efflux is approximately equal to the rate of H^+ uptake. We observe, in agreement with most other workers, that the passive H^+ back-flux into the matrix exhibits a highly non-linear dependence on protonmotive force (pmf). We propose that the nonlinearity is not due to changes in H^+ permeability, as is generally assumed; rather it is due to the fact that the driving forces are so large that we are outside the range of linearity between fluxes and forces. At the high forces normally achieved in mitochondria (>100 mV), we move into the range of validity of another approximation, according to which the logarithm of the flux is linear with pmf. This analysis provides new information on the nature of electrophoretic ion transport in mitochondria. Thus, at all values of pmf, proton transport behaves like diffusion across a high energy barrier within an insulating membrane. We find no evidence for carrier mediation or regulation of proton transport or of dielectric breakdown at high values of pmf. We obtain a constant value for the proton permeability of the inner membrane (about 10^{-4} cm/s or 0.2 nmol mg^{-1} min^{-1}) over the entire range of pmf studied, between 130 and 220 mV. This research was supported by N.I.H. grants GM 31086 and HL 36573.

M-AM-G4 REGULATION OF THE MITOCHONDRIAL ATPase IN SLOW AND FAST HEART-RATE HEARTS: ROLE OF Pi/H^+ SYMPORT. William Rouslin and Charles W. Broge, Department of Pharmacology and Cell Biophysics, University of Cincinnati College of Medicine, Cincinnati, Ohio 45267-0575.

Earlier studies by us demonstrated that inhibitor protein binding to the mitochondrial ATPase in intact, non-energized cardiac muscle mitochondria is governed primarily by matrix pH (Rouslin, W., J. Biol. Chem. 262: 3472-3476, 1987). Other studies by us showed that this protonic inhibition of the mitochondrial ATPase which occurs *in situ* in ischemic (non-energized and acidotic) hearts is evident only in so-called slow heart-rate hearts (HRH), i.e., hearts with heart rates of approximately 200 beats/min or less (Rouslin, W., Am. J. Physiol. 252: H622-H627, 1987). Only a slight *in situ*, ischemia-induced ATPase inhibition can be demonstrated in so-called fast HRH, i.e., those with heart rates of approximately 300 beats/min or more. Our work has also suggested that this lack of *in situ* ATPase inhibition in fast HRH may be due to an insulation of the fast HRH mitochondria against the cytosolic acidosis which develops during ischemia in all of the species studied by us. Our most recent work, to be presented here, shows that intact mitochondria from both slow and fast HRH are capable of maintaining a blockade to external H^+. However, slow HRH mitochondria appear to have a very low threshold blockade to external H^+ which appears to be regulated by Pi which accumulates rapidly in ischemic cardiac muscle cells. In contrast, fast HRH mitochondria appear to have a firm blockade to external H^+ which is unaffected by Pi. We shall present data suggesting that Pi/H^+ symport is the primary process by which H^+ pass to the matrix space causing matrix acidification and, therefore, ATPase inhibition during ischemia in slow HRH but not, apparently, in fast HRH. (Supported by NIH grant HL30926-04 and by grants from the American Heart Association, Southwestern Ohio Affiliate.)

M-AM-G5 PATCH CLAMP STUDIES OF THE INNER MITOCHONDRIAL MEMBRANE REVEAL A VOLTAGE DEPENDENT ION CHANNEL. B.U. Keller[+], M.C. Sorgato[¶], W. Stühmer[+]
[+]Max-Planck-Institut f. biophys. Chemie, D-3400 Göttingen, F.R.G. and
[¶]Instituto di Chimica Biologica e Centro CNR per lo Studio della Fisiologia Mitochondriale, I-35131 Padova, Italy.

Patch clamp studies were carried out on the inner membrane of mitochondria isolated from mouse liver. For this, giant mitochondria were obtained from cuprizone fed mice and isolated according to the protocol of Hochman et al., Biochemistry 24, 2509-2516 (1985). Outer mitochondrial membranes were removed by osmotic swelling and sonication, yielding inner membrane vesicles (mitoplasts) of 3-6 µM in diameter. Standard patch clamp measurements of the inner mitochondrial membrane (IMM) reveal a voltage dependent ion channel which has not been previously described. The occurrence of 1-4 channels in most membrane patches suggests a relative abundance of the channel in the IMM. Single channel conductance is 107 pS in 150 mM KCl with Cl^- being about five times more permeable than K^+. Channel gating is strongly voltage dependent. Under resting potential conditions (-180 mV across the IMM, mitoplast inside negative), the channel is permanently closed. This applies for pH values ranging from 6.2 to 9.0 on either side of the IMM. Channel openings occur at voltages positive to -30 mV and they dominate the gating behaviour for voltages V > +40 mV. The physiological importance of the IMM channel is discussed.

M-AM-G6 "Spatial organization of redox active centers in the Bovine Heart Ubiquinol-cyt. *c* oxidoreductase." T. Ohnishi, S.W. Meinhardt, R. LoBrutto, and G. Von Jagow* Dept. of Biochem. & Biophys., Univ. of Penn. Phila., PA 19104 *Physikalische Biochemie der Univ. MÜnchen, MÜnchen, FRG

To examine the spatial organization of cyt. b_{562}, b_{566}, c_1 hemes, and the Rieske iron-sulfur cluster, we have analyzed spin-spin interactions between intrinsic redox centers, and between intrinsic centers and extrinsic probes. By appropriately redox-poising the stigmatellin treated Complex III, we have detected about 40% enhancement of the $P_{1/2}$ of the cluster by each c_1 and b_{566} spins, but not by b_{562}. Using the spin probe approach, we measured the effective distances of the redox centers from both surfaces of the reconstituted proteoliposomes. We have improved our model system through the use of liposomes into which is incorporated stearic acid spin-labelled at different carbon positions. We obtained a r^{-4} dependence in their T_1 enhancement by extrinsic probes. Combined data show that (See the figure) the Rieske cluster is located close to the outer surface of the phospholipid bilayer if the cluster is in the central region of Complex III. The cyt. b_{562} heme is located at a depth of approximately 40% of the bilayer thickness from the C-side. The effect of Dysprosium on cyt. b_{566} from the C-side surface gave about the same effective distance as Rieske clusters, but no probe effect was detected from the M-side surface because of the extremely rapid intrinsic relaxation rate of cyt b_{566}. These results are in good agreement with the topological distribution reported using other methods (Supported by NSF DMB 85-11160).

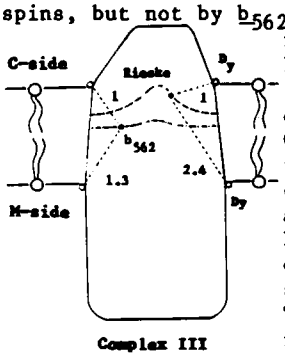

Complex III

M-AM-G7 SPECTROSCOPIC CHARACTERIZATION OF PURIFIED UBIQUINOL:CYTOCHROME c_2 OXIDOREDUCTASE FROM *Rhodobacter sphaeroides*

Katherine M. Andrews, Antony R. Crofts*, and Robert B. Gennis, Department of Biochemistry and Department of Physiology and Biophysics*, University of Illinois, Urbana, Illinois, 61801.

A highly active preparation of ubiquinol:cytochrome c_2 oxidoreductase has been characterized by UV-visible and EPR spectroscopy. The complex catalyzes the reduction of horse heart cytochrome *c* with a turnover in excess of 300 mol s^{-1} (mol c_1)$^{-1}$ and contains two thermodynamically distinct *b* cytochromes and cytochrome c_1 with midpoint potentials similar to those found in chromatophores. Redox titrations of the Rieske iron-sulfur cluster were monitored by EPR at 15 K and show an E_m value of +275 mV (vs. SCE) in the absence of inhibitor. In the presence of UHDBT the E_m value of the iron-sulfur cluster was shifted to +315 mV, and the g_x, g_y and g_z values were shifted. The shape of the high-field line was shown to be sensitive to the redox state of the system and to the presence of UHDBT. These results are similar to those observed in the mitochondrial complex and in purified bc_1 from *Paracoccus denitrificans* (Meinhardt, S.W., Yang, X., Trumpower, B.L., and Ohnishi, T. (1987) *J. Biol. Chem.* 262, 8702-8706). Properties of the thermodynamically stable ubisemiquinone, Q_i, have also been studied in the purified complex. The radical is antimycin-sensitive and has an isotropic signal centered at g=2.0035. The pH dependence of the midpoint potential and magnitude of the semiquinone signal will be presented. The thermodynamically unstable ubisemiquinone, Q_o, which can be generated by oxidant-induced reduction of cytochrome *b*, is also being studied. We are currently working on further characterization of Q_i by ENDOR and ESEEM techniques. This work was supported by NIH grants PHS R01 GM 26305 and GM 35438. Instrumentation was provided by the University of Illinois ESR Research Center (NIH RR 01811).

M-AM-G8 EPR Characterization of the NADH Ubiquinone Oxidoreductase of Photosynthetically Grown Rhodobacter capsulatus. Steven W. Meinhardt and Tomoko Ohnishi, Department of Biochemistry and Biophysics, University of Pennsylvania, Philadelphia, PA 19104

In chromatophores of photosynthetically grown Rd. capsulatus, we have identified five distinct iron-sulfur clusters which are not associated with the cytochrome bc_1 and succinate dehydrogenase complexes. Redox titrations of the g = 1.94 signal measured at a sample temperature of 25K and a microwave power of 2 mW shows three binuclear iron-sulfur clusters with redox midpoint potentials of -340, -100 and +46 mV, pH 7. The highest potential component appears to be S-1 of the succinate dehydrogenase. Titration curves from the g = 1.92 signal measured at 11K, 5 mW shows three apparently tetranuclear iron-sulfur clusters with midpoints of -240, -130 and -4 mV, pH 7. Although the iron-sulfur clusters exhibited low signal amplitudes the $g_{x,y}$ portion of the spectra have been partially resolved. Both binuclear clusters exhibited axial spectra with g = 1.94. The two lowest potential tetranuclear clusters have rhombic spectra, $g_{x,y}$ = 1.92, 1.94, while the highest potential tetranuclear clusters has an apparently axial spectrum with g = 1.92. No resolution of the g_z peaks could be obtained. Substrate reduction indicates that at least one binuclear and one tetranuclear cluster are part of the NADH dehydrogenase. We will also present data from the study NADH dehydrogenase mutants and specific inhibitors of the NADH ubiquinone oxidoreductase system. This research is supported by NIH Grant GM 30736.

M-AM-G9 Chemical and Spectroscopic Evidence for the Formation of a Ferryl Fe_{a3} Intermediate in H_2O_2-treated Cytochrome c Oxidase

S.N. Witt, J. Manthey, and S.I. Chan, Department of Chemistry, California Institute of Technology Pasadena, CA 91125
R. Kean, J. Centano, H. Fonda, and G.T. Babcock, Department of Chemistry, Michigan State Univ., East Lansing, MI 48824-1322

Upon the addition of excess hydrogen peroxide to reduced (or pulsed) cytochrome c oxidase, a homogeneous population of a reactive EPR-silent, three-electron-reduced intermediate is trapped at the dioxygen reduction site. The optical spectrum of the species is characterized by a Soret maximum at 428 nm and an alpha band at 595-596 nm, with alpha and beta bands at 580 and 535 nm in the reoxidized minus resting difference spectrum, respectively. When an equivalent of NADH is added to the 428/580 nm species, the pulsed enzyme is produced in high yield as judged by the appearance of the unusual EPR resonances at g=5, 1.8, and 1.7; thus, the 428/580 nm species contains more oxidizing equivalents than the pulsed enzyme. In addition, we recently characterized the 428/580 nm species by resonance Raman spectroscopy. The oxidation state marker band (ν_4 = 1377 cm^{-1}) and the spin-state marker band (ν_2 = 1595 cm^{-1}) are consistent with an intermediate-spin ferryl Fe_{a3}. These combined chemical and spectroscopic results demonstrate that H_2O_2 activates cytochrome c oxidase to produce a ferryl Fe_{a3}/cupric Cu_B binuclear couple at the dioxygen reduction site.

M-AM-G10 Cytochrome c Oxidase Exhibits a Rapid Conformational Change upon Reduction of Cu_A. Robert A. Copeland, Paul A. Smith, Thomas Nilsson, Sunney I. Chan. Arthur Amos Noyes Laboratory of Chemical Physics, California Institute of Technology, Pasadena, California 91125.

When cytochrome c oxidase is reduced, it undergoes a conformational change that shifts its tryptophan fluorescence maximum from 329 to 345 nm. This red shift appears to be due to increased solvent exposure of the tryptophan residues, as Cs^+ quenches the fluorescence of the reduced enzyme (with a Stern-Volmer constant of 0.69) while the oxidized enzyme shows no quenching. Studies of ligand-bound, mixed valence forms of cytochorme c oxidase show that the tryptophan fluorescence change is associated with reduction of the two low-potential metal centers, cytochrome a and Cu_A. The previously proposed "open-closed" transition monitored by changes in cyanide binding kinetics also depends on the redox state of the low-potential centers. To determine how these conformational transitions depend on reduction of cytochrome a and/or Cu_A, a reductive titration of the cyanide inhibited enzyme was compared with a theoretical model based on the difference in redox potentials between the two centers and their known anticoopertivity. Both indicators of conformational change correlate best with reduction of Cu_A. Derivatives of the enzyme were prepared in which the Cu_A site is modified. Perturbation of Cu_A eliminates both the redox-linked tryptophan fluorescence change and the open-closed transition. The significance of these conformational changes with respect to the proton pumping mechanism of cytochrome c oxidase will be discussed.

M-AM-G11 SITE-DIRECTED MUTAGENESIS OF THE BETA SUBUNIT OF F_1-ATPase. M.K. Al-Shawi, D. Parsonage and A.E. Senior, Dept. Biochemistry, Univ. of Rochester Medical Center, Rochester, NY 14642

Directed mutagenesis was used to substitute Asn or Val for Asp-242 of the β-subunit of Escherichia coli F_1-ATPase. Asp-242 is highly conserved in F_1-β subunits in a region of sequence which shows homology with several nucleotide-binding proteins. By analogy with adenylate kinase, it has been suggested (Fry et. al. (1986) PNAS 83 907-911) that Asp-242 might participate during ATP synthesis and hydrolysis by F_1 either through electrostatic effects on the substrate Mg^{2+}, or through hydrogen-bonding to the substrate water. The substitutions chosen affect the charge, hydrogen-bonding ability and hydrophobicity of residue β-242. Both substitutions impaired ATP synthesis in vivo, and reduced ATPase and ATP-driven proton pumping activities in vitro by 90% (Asn-242) and 80% (Val-242). The purified mutant F_1-ATPases had normal molecular size, subunit composition and stability. The relative "multisite" activities of the mutant enzymes were similar in pH profile to normal. Relative differences in CaATPase vs MgATPase were minor. Analyses of "unisite" kinetics revealed that the elementary steps of catalysis were largely unaffected by the substitutions, except that K_dATP at the high-affinity site was much-reduced. K_dADP was unchanged. Promotion of catalysis was attenuated. It is concluded that residue β-242 is essential and is required for cooperative interactions between the F_1 catalytic sites. However, residue β-242 does not seem to play a critical role in bond cleavage-bond formation in catalysis. The results are consistent with the hypothesis that high-affinity ATP-binding, reversible ATP synthesis at the first catalytic site and positive cooperativity all require exact stereochemical orientation of substrates and products in the catalytic site.

M-AM-G12 RANDOM MUTAGENESIS OF THE BETA-SUBUNIT OF F_1-ATPase. F.A.S. Kironde, D. Parsonage and A.E. Senior. Dept. of Biochemistry, University of Rochester Medical Center, Rochester, NY 14642

The uncD gene encoding the β-subunit of Escherichia coli F_1-ATPase was cloned in suitable vectors and mutagenised with hydroxylamine or nitrosoguanidine. The following β-subunit mutations were identified by DNA sequencing: (1) Cys-137→ Tyr; (2) Gly-142→ Asp; (3) Gly-207→ Asp; and (4) Pro-403→ Ser, Gly-415→ Asp (double mutation). It was confirmed that the rest of the uncD gene sequence was normal in each case. Each of the mutations caused reduced ATP synthesis in vivo as measured by growth on succinate or limiting (3mM) glucose, and caused reduced ATPase and ATP-driven proton-pumping in membranes in vitro. The first three mutations lie in a region of sequence previously predicted to form the catalytic nucleotide-binding domain in β-subunit. The effects of these mutations on catalysis may therefore be similar to those seen in β-subunit mutants previously reported. The double mutant (#4 above) is interesting because the amino acid substitutions lie outside the predicted nucleotide-binding domain, close to Ser-413, the residue equivalent to the site of FSBA-labelling at low pH (Bullough and Allison, J. Biol. Chem. 261 5722-5730, 1986). This suggests that the region of β-subunit between residues 403 and 415 may be involved in an α/β subunit interface. Analysis of revertants is underway to determine whether Pro-403 or Gly-415 (or both) is the functionally-important residue in the double-mutant.